

| | | | | | |
|--|--|---|--|---|-----------|
| 1. Report No. FHWA/TX-97/1341-2 | | 2. Government Accession No. | | 3. Recipient's Catalog No. | |
| 4. Title and Subtitle USING ELECTRICAL PROPERTIES TO CLASSIFY THE STRENGTH PROPERTIES OF BASE COURSE AGGREGATES | | | | 5. Report Date November 1995 Resubmitted: July 1996 | |
| | | | | 6. Performing Organization Code | |
| 7. Author(s) Timo Saarenketo and Tom Scullion | | | | 8. Performing Organization Report No. Research Report 1341-2 | |
| 9. Performing Organization Name and Address Texas Transportation Institute The Texas A&M University System College Station, Texas 77843-3135 | | | | 10. Work Unit No. (TRAVIS) | |
| | | | | 11. Contract or Grant No. Study No. 0-1341 | |
| 12. Sponsoring Agency Name and Address Texas Department of Transportation Research and Technology Transfer Office P. O. Box 5080 Austin, Texas 78763-5080 | | | | 13. Type of Report and Period Covered Interim: September 1994 - August 1995 | |
| | | | | 14. Sponsoring Agency Code | |
| 15. Supplementary Notes Research performed in cooperation with the Texas Department of Transportation and the U.S. Department of Transportation, Federal Highway Administration. Research Study Title: Using Ground Penetrating Radar | | | | | |
| 16. Abstract <p>Eight different types of Texas aggregates and three Finnish aggregates were tested in order to relate their dielectric value and electrical conductivity, measured at different moisture contents and densities, to their strength and deformation properties. The dielectric value and electrical conductivity were measured in the laboratory using a surface probe and dielectric meter. The real and imaginary part of the dielectric value of aggregate fines were measured with a Surface Network Analyzer over a frequency range from 30 MHz to 3.0 GHz. Aggregate strength properties were obtained using a Dynamic Cone Penetrometer (DCP) and Resilient Modulus Tests. Aggregate suction properties and their behavior during the freeze/thaw cycles were monitored with a special Tube Suction Test and Freeze/Thaw Test developed by the authors.</p> <p>The purpose of this study was to evaluate what range of dielectric values and electrical conductivities can be expected when processing and interpreting Ground Penetrating Radar (GPR) survey results. Dielectric values affect the radar signal velocity and the time/thickness scale of radar profile. It was also hoped to determine if these dielectric properties of aggregates correlate with their strength and deformation properties of these materials.</p> <p>The result of the study showed that the dielectric value and electrical conductivity related to both the strength and deformation properties and frost susceptibility of base course aggregates. The dielectric value correlates well with the California Bearing Ratio (CBR)-value of compacted base materials. Low dielectric values (5.5 - 6.5) in compacted samples indicate the presence of thin and well-arranged adsorption water and optimum strength properties. Higher values indicate that material is sensitive to moisture, and dielectric values over 9 - 10 are "alarm values" because they can have unfrozen water in their structure when the material freezes. If the dielectric value is greater than 16 the base material will become plastic and deformation will occur in the structure. High electrical conductivity values indicate high amounts of ions dissociated to the free water, and this can cause positive pore pressure in base materials. Saturation hysteresis was also found to have a substantial effect on base strength.</p> | | | | | |
| 17. Key Words Ground Penetrating Radar, Dielectric, Base Courses, Aggregates, Moisture Susceptibility | | | 18. Distribution Statement No restrictions. This document is available to the public through NTIS: National Technical Information Service 5285 Port Royal Road Springfield, Virginia 22161 | | |
| 19. Security Classif.(of this report) Unclassified | | 20. Security Classif.(of this page) Unclassified | | 21. No. of Pages 87 | 22. Price |

**USING ELECTRICAL PROPERTIES TO CLASSIFY THE
STRENGTH PROPERTIES OF BASE COURSE AGGREGATES**

by

Timo Saarenketo
Finnish National Road Administration
Road District of Lapland

and

Tom Scullion
Texas Transportation Institute
Texas A&M University

Research Report 1341-2
Research Study Number 0-1341
Research Study Title: Using Ground Penetrating Radar

Sponsored by the
Texas Department of Transportation
In Cooperation with
U.S. Department of Transportation
Federal Highway Administration

November 1995
Resubmitted: July 1996

TEXAS TRANSPORTATION INSTITUTE
The Texas A&M University System
College Station, Texas 77843-3135

IMPLEMENTATION STATEMENT

The Texas Department of Transportation (TxDOT) has purchased a Ground Penetrating Radar (GPR) system and currently offers routine services to Districts. Current efforts have focused on measuring the properties of the top layer, which is normally asphaltic concrete. The results of this study indicate that the GPR data can also be used to infer meaningful engineering properties for granular base layers.

DISCLAIMER

The contents of this report reflect the views of the authors who are responsible for the facts and the accuracy of the data presented herein. The contents do not necessarily reflect the official view or policies of the Texas Department of Transportation (TxDOT) or the Federal Highway Administration (FHWA). This report does not constitute a standard, specification, or regulation, nor is it intended for construction, bidding, or permit purposes. The engineer in charge of the project was Tom Scullion, P.E. #62683.

ACKNOWLEDGMENT

This work has been conducted with the support of the Texas Department of Transportation (TxDOT), the Federal Highway Administration (FHWA) and the Road District of Lapland of the Finnish National Road Administration. Mr. Harold Albers from TxDOT helped in selecting and collecting test materials and gave useful advice. Mr. Joel Colwell provided great assistance with the laboratory testing and data processing.

TABLE OF CONTENTS

| | Page |
|---|-------------|
| List of Figures | xi |
| List of Tables | xiv |
| Summary | xv |
| Chapter 1 Introduction | 1 |
| Chapter 2 Theory | 3 |
| 2.1 Factors Affecting Aggregate Strength and Deformation Properties | 3 |
| 2.2 Water in Frozen and Unfrozen Aggregates | 5 |
| 2.3 Dielectric Value and Electrical Conductivity | 7 |
| 2.4 Ground Penetrating Radar and Other Techniques in Monitoring Base Moisture Content | 11 |
| Chapter 3 Materials and Study Methods | 15 |
| 3.1 Aggregates, Lithology and Grading | 15 |
| 3.2 Aggregate Fines | 17 |
| 3.3 Dielectric Value, Electrical Conductivity Measurements and DCP - Tests | 21 |
| 3.4 Resilient Modulus Tests | 24 |
| 3.5 Tube Suction Tests | 26 |
| 3.6 Freezing Test | 28 |
| Chapter 4 Results and Discussion | 29 |
| 4.1 Previous Surveys with Finnish Aggregates | 29 |
| 4.2 Electrical Properties of Aggregate Fines | 29 |
| 4.3 Relation Between Dielectric Value and Electrical Conductivity and Moisture Content | 35 |
| 4.4 Compaction Degree, Degradation and Solubility | 38 |
| 4.5 DCP- and Resilient Modulus Tests | 42 |
| 4.6 Tube Suction Test Results | 48 |
| 4.7 Freeze/Thaw Effect to the Aggregate Properties | 55 |

| | |
|---|----|
| Chapter 5 Conclusions and Classification of Base Aggregates According to Their Electrical Properties | 59 |
| References | 63 |
| Appendix - Grain Size Distribution Curves of Tested Texas Aggregates | 69 |

LIST OF FIGURES

| | | Page |
|-----|--|-------------|
| 1. | Relationship Between Volumetric Water Content and Matric Suction (Modified After Fredlund and Rahardjo, 1993) | 4 |
| 2. | The Structure of Adsorption Water | 6 |
| 3. | Adsorption Water in Loose Compacted and Frozen Micro Structures | 8 |
| 4. | Calculating Layer Dielectrics Using the Surface Reflection Method. (Maser and Scullion, 1991) | 12 |
| 5. | Grain Size Distribution of <0.074 mm (<200 mesh) Fraction of the Test Base Aggregates. Analysis was Made with Micromeritics Sedigraph | 18 |
| 6. | Comparison of Fine Fraction Properties of the Test Aggregates Together with the Finnish Base Course Materials Fine Fraction Study Results. The Finnish Materials have Classified as Felsic and Mafic Aggregates. Felsic Aggregates are Dominated with Granitoid and Mafic Aggregates have Higher Ferromagnesian Minerals Content | 20 |
| 7. | Correlation Between Water Adsorption and Clay Content in the Fine Fraction of the Test Aggregates | 22 |
| 8. | Dielectric Tube Probe of Dielectric and Electrical Conductivity Meter, Proctor Hammer and Test Bucket Used in the Test | 23 |
| 9. | Tube Suction Test Arrangements | 27 |
| 10. | Dielectric Value at Different Gravimetric Moisture Contents of Finnish Aggregates. Filled Square and Triangle Represent Moisture Sensitive Aggregates with High Water Adsorption Values, which are Presented after Aggregate Names | 30 |
| 11. | Correlation of Dielectric Value and Volumetric Water Content of Two Types of Finnish Base Aggregates | 31 |
| 12. | Real Part (K') of Dielectric Value of Three Different Types of Aggregate Base Fines. Measurements with Surface Network Analyzer Surface Probe Have Been Made from Oven Dry Samples and Samples Balanced with 100 % Relative Air Moisture at Room Temperature | 33 |

| | | |
|-----|--|----|
| 13. | Imaginary Part (K'') of Dielectric Value of Three Different Types of Aggregate Base Fines. Measurements with Surface Network Analyzer Surface Probe Have Been Made from Oven Dry Samples and Samples Balanced with 100 % Relative Air Moisture at Room Temperature | 34 |
| 14. | Correlation Between Dielectric Value and Gravimetric Moisture Content of Texas Aggregates | 36 |
| 15. | Correlation Between Electrical Conductivity and Gravimetric Moisture Content of Texas Aggregates | 37 |
| 16. | Moisture vs. Dry Density Relation of Different Types of Uncompacted Test Aggregates. Water Adsorption Values are Also Marked to Each Moisture-Density Curve | 39 |
| 17. | Moisture vs. Dry Density Relation of the Compacted Aggregates Presented in Figure 16 | 40 |
| 18. | The Increase of Fines of Test Aggregates During the Compaction Test | 41 |
| 19. | Correlation Between CBR-Value and Gravimetric Moisture Content of the Test Aggregates. Grey Squares Present Texas Carbonate Aggregates, Black Squares Other Texas Aggregates and Open Diamonds Finnish Aggregates | 43 |
| 20. | Correlation Between CBR-Value and Dielectric Value of Texas and Finnish Test Aggregates. Grey Squares Present Texas Carbonate Aggregates, Black Squares Other Texas Aggregates and Open Diamonds Finnish Aggregates | 44 |
| 21. | Correlation Between CBR-Value and Electrical Conductivity of Texas and Finnish Aggregates. Grey Squares Present Texas Carbonate Aggregates, Black Squares Other Texas Aggregates and Open Diamonds Finnish Aggregates | 45 |
| 22. | The Effect of Saturation and Drying in the Strength Properties and Dielectric Value of Some Texas Carbonate Aggregates | 47 |
| 23. | Correlation Between Dielectric Value and Resilient Modulus Calculated from Dynamic Triaxial Test of Test Aggregates | 49 |
| 24. | Dielectric Value Distribution Curve of Tube Suction Test of a Medium Grained Texas River Sand | 50 |
| 25. | Electrical Conductivity Distribution Curve of Tube Suction Test of a Medium Grained Texas River Sand | 51 |

| | | |
|-----|---|----|
| 26. | Dielectric Surface Probe and the Results From the Suction Test | 53 |
| 27. | The Effect of Gradation to the Suction Properties of Samples #2 Granite/Basalt and #14 Tohmo Granite | 54 |
| 28. | Correlation Between Dielectric Values of Unfrozen and Frozen Base Aggregates | 56 |
| 29. | Correlation Between Electrical Conductivity Values of Unfrozen and Frozen Base Aggregates | 57 |
| 30. | Dielectric Values of the Test Aggregates Before, During and After the Samples were Frozen at the Temperature of -5°C | 58 |
| A1. | Grain Size Distribution of Texas Aggregates #1-4 | 70 |
| A2. | Grain Size Distribution of Texas Aggregates #5-8 | 71 |

LIST OF TABLES

| | Page |
|--|-------------|
| 1. Fine Fraction Properties of Test Materials | 19 |
| 2. Real and Imaginary Part of the Dielectric for the Study Aggregate After Water Adsorption | 32 |
| 3. Resilient Modulus Test Results of the Test Aggregates | 48 |
| 4. Classification of Base Aggregates According to Their Electrical Properties | 61 |

SUMMARY

Eight different types of Texas aggregates and three Finnish aggregates were tested in order to relate their dielectric value and electrical conductivity, measured at different moisture contents and densities, to their strength and deformation properties. The dielectric value and electrical conductivity were measured in the laboratory using a surface probe and dielectric meter. The real and imaginary part of the dielectric value of aggregate fines were measured with a Surface Network Analyzer over a frequency range from 30 MHz to 3.0 GHz. Aggregate strength properties were obtained using a Dynamic Cone Penetrometer (DCP) and Resilient Modulus Tests. Aggregate suction properties and their behavior during the freeze/thaw cycles were monitored with a special Tube Suction Test and Freeze/Thaw Test developed by the authors.

The purpose of this study was to evaluate what range of dielectric values and electrical conductivities can be expected when processing and interpreting Ground Penetrating Radar (GPR) survey results. Dielectric values affect the radar signal velocity and the time/thickness scale of radar profile. It was also hoped to determine if these dielectric properties of aggregates correlate with their strength and deformation properties of these materials.

The result of the study showed that the dielectric value and electrical conductivity related to both the strength and deformation properties and frost susceptibility of base course aggregates. The dielectric value correlates well with the California Bearing Ratio (CBR)-value of compacted base materials. Low dielectric values (5.5 - 6.5) in compacted samples indicate the presence of thin and well-arranged adsorption water and optimum strength properties. Higher values indicate that material is sensitive to moisture, and dielectric values over 9 - 10 are "alarm values" because they can have unfrozen water in their structure when the material freezes. If the dielectric value is greater than 16 the base material will become plastic and deformation will occur in the structure. High electrical conductivity values indicate high amounts of ions dissociated to the free water, and this can cause positive pore pressure in base materials. Saturation hysteresis was also found to have a substantial effect on base strength.

CHAPTER 1

INTRODUCTION

The background of this study relates to the history of the Ground Penetrating Radar (GPR) applications in road surveys. In Finland the method has been used in road surveys since 1986 covering various fields of application from site investigations to aggregate exploration and from concrete bridge deck deterioration mapping to road structural course thickness surveys and investigation of damage (Saarenketo 1992, Saarenketo and Söderqvist 1993, Maijala et al. 1994). In Texas the GPR applications in roads have mainly measured thicknesses of the pavement and base layers (Maser et al. 1991, Maser and Scullion 1991), but recently efforts have been made to apply GPR technique in detecting subsurface defects such as stripping and voids or locating sinkholes beneath the highway structure (Scullion et al. 1992, Lau et al. 1992, Saarenketo and Scullion 1994). GPR equipment is now widely available. The Texas Department of Transportation (TxDOT) has purchased a 1 GHz air-launched horn antenna for rapidly surveying pavement structures.

The two basic material properties affecting the propagation of radar signals in road structures and subgrade soils are the dielectric value and electrical conductivity. The dielectric value of each road layer has to be estimated in order to calculate the thickness of the layer. As there were data already available on the dielectric properties of subgrade soils (Campbell 1990, Sutinen 1992), but no data on base course materials, there was a need to investigate what range of dielectric values and electrical conductivities can be expected. Also there was interest in identifying the relationship between dielectric value and electrical conductivity and the actual volumetric or gravimetric moisture content of base materials.

Another reason for these tests was the observation made in Finland that there seemed to be a correlation between low spring bearing capacity and a certain type of GPR reflection pattern from base courses. These relationships were noted even during the dry summer months when the road section was its strongest. This special "ringing type" reflection pattern could not be explained by any reason other than changes in the dielectric properties of the base material.

A final reason for this study was to test the observation gained from the GPR survey data in Finland that there seemed to be a very good correlation between the dielectric properties and

strength and deformation properties of all types of soils and aggregates, i.e., the higher the dielectric value, the lower the bearing capacity. Mitchell (1992) documents the idea of this relationship as he writes "As the strength of a soil depends in part on interparticle attractions, it would be expected that the strength would also be influenced by dielectric constant."

CHAPTER 2

THEORY

2.1. FACTORS AFFECTING AGGREGATE STRENGTH AND DEFORMATION PROPERTIES

Water, to a greater or lesser extent, affects the mechanical properties of all pavement materials and soils. However the magnitude of these effects depends on the material properties, moisture content and even on the saturation history of the layer. Both positive and negative pore-water pressures in a soil have a major effect on shear strength and volume change (Fredlund et al. 1995). When discussing the negative pore-water pressure, the term "suction" is used for the thermodynamic quantity, Gibbs free energy which generates tension in the pore water between soil particles (Lytton 1994). The total suction is composed of two components: 1. matric suction and 2. osmotic suction (Fredlund and Rahardjo 1993).

In low moisture content base materials, suction can increase the resilient modulus of aggregates (see Thom 1988 and Sweere 1990), but when the moisture content increases the effect of suction decreases (Fredlund and Rahardjo 1993). At high moisture contents, positive pore water pressure can decrease the base material resistance to recoverable and irrecoverable deformations (Kolisoja 1993).

Hysteresis, the effect of wetting and drying, has an influence to the amount of suction in soils (Fredlund and Rahardjo 1993). The matric suction is higher at a particular volumetric water content when the material is drying than at the same water content when it is wetting (Figure 1).

The freeze/thaw process can also have a dramatic influence on the recoverable and irrecoverable deformation of base materials. The grain size, pore size and total internal surface area of rock aggregates have a major influence not only on the freeze/thaw durability, but also on the wetting-drying resistance and overall durability of aggregate (Hudec and Achampong 1994). The freeze/thaw process together with dynamic traffic load can cause rapid disintegration of base course material with high specific surface area (Saarenketo and Nieminen 1989), and there is also clear evidence of a correlation between thermal cracking on pavements and

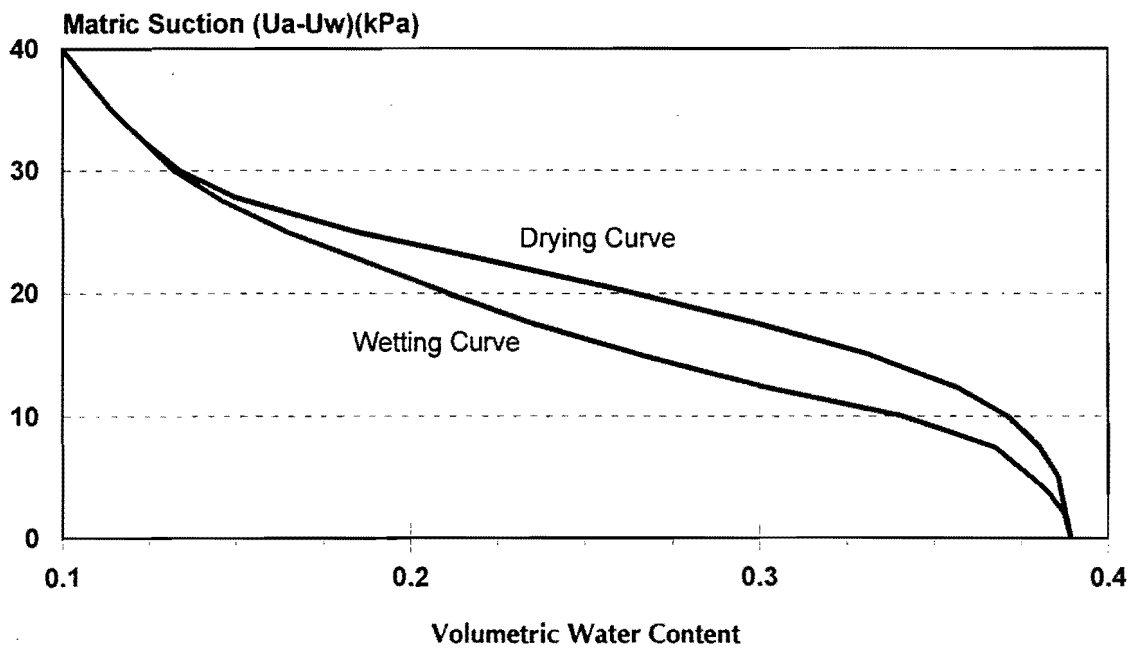


Figure 1. Relationship Between Volumetric Water Content and Matric Suction (Modified After Fredlund and Rahardjo, 1993).

freeze/thaw cycling properties of high water adsorbing base course aggregates in Texas (Carpenter and Lytton 1977).

2.2. WATER IN FROZEN AND UNFROZEN AGGREGATES

Water can exist in soils in either

- a. the crystalline structures of minerals,
- b. as free water, or
- c. as bound water.

Bound water consists of adsorption and viscous water layers. In adsorption water, the dipole water molecules closest to the mineral surface are systematically arranged towards the mineral surface that has a negative charge (Figure 2). This approximately 10 - 20 Å thick layer (Mitchell 1992) has higher density and is also tightly bound. Its structure has been suggested to be nearly tetrahedral (Mitchell 1992). The outer adsorption water layer around a soil particle is called the loosely bound layer. The bonding force decreases with the distance from the mineral surface, and outer layers of adsorption water are very sensitive to the changes of air pressure and temperature.

The water molecule adsorption layer also has ions which are attracted to the negative corners of water molecules or to the mineral surface. According to Mitchell (1992) possible bonding mechanisms of the water adsorption by mineral surfaces are

- a. hydrogen bonding,
- b. ion hydration,
- c. attraction by osmosis, and
- d. dipole attraction.

Between adsorption water and free gravitational water there is another type of bound layer, which can be called viscous or capillary water. Viscous water differs from adsorption water in that it cannot adsorb water from the air, and unlike adsorption water, evaporation can reduce its volume during the warm and dry seasons.

STRUCTURE OF ADSORPTION WATER

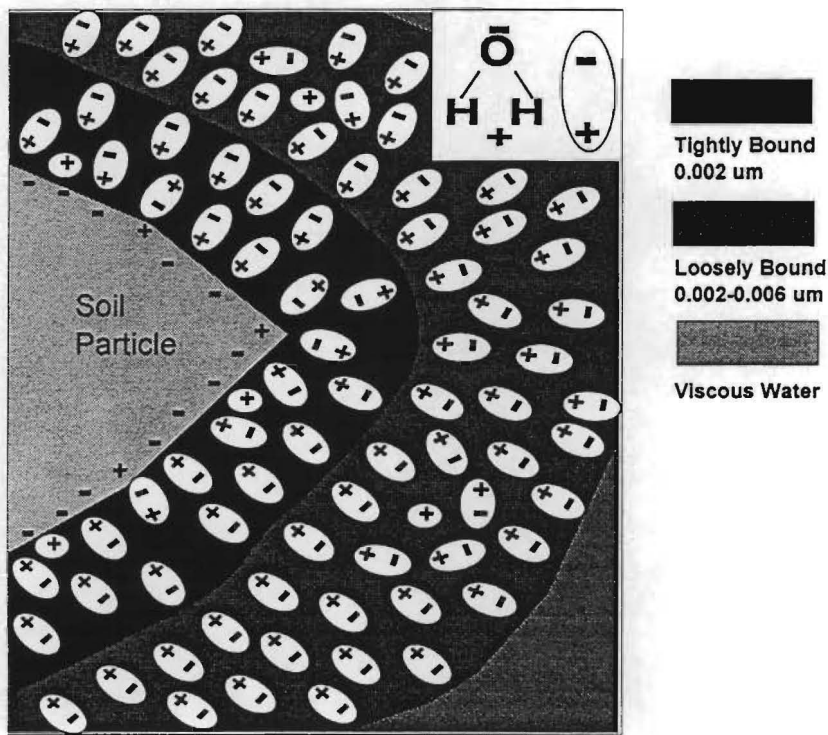


Figure 2. The Structure of Adsorption Water.

When soil temperature drops below 0°C, free water forms hexagonal crystals and thus expands in volume (Tsytovic 1986). During the freezing process, water molecules add one by one to the growing ice crystals, but they remain separated from the mineral surface by the thin adsorption layer (Anderson 1989). The “Frozen Fringe” is the relatively narrow area below the nominal base of the ice lens (Ladanyi and Shen 1989). At the same time suction causes liquid water to migrate to the ice lens from the unfrozen soil through this unfrozen water layer (Konrad and Morgenstern 1980).

As the temperature in the soil continues to decrease the bound water starts to freeze, but the tightly bound layer remains unfrozen (Figure 3). At a temperature of -5°C the amount of unfrozen water is still 12% of the total volume of unfrozen water (Anderson 1989). The amount of the frozen adsorption water decreases with decreasing temperature until the water movement to the frozen fringe is significantly reduced. Small amounts of unfrozen water in soil have been measured even at temperatures of -40°C (Anderson 1989).

The amount of dissolved salts, relict salt and the byproducts of hydrolytic reactions also control the freezing process, which according to Kujala (1991) lowers the amount of free energy and thus lowers the freezing temperature. On the other hand many fine-grained base aggregates such as argillaceous carbonates, volcanites, sandstones and chert and shale impurities degrade with repeated wetting and drying and with freezing and thawing, especially under the influence of de-icing salts (Hudec and Achampong 1994).

2.3. DIELECTRIC VALUE AND ELECTRICAL CONDUCTIVITY

If magnetic permeability is neglected, earth materials can be characterized by their electrical conductivity and dielectric permittivity ϵ , that is in general a complex function of frequency.

The relative dielectric permittivity K (dielectric constant) is defined as

$$K = \epsilon / \epsilon_0$$

where ϵ_0 is free space permittivity, dielectric constant can be expressed by

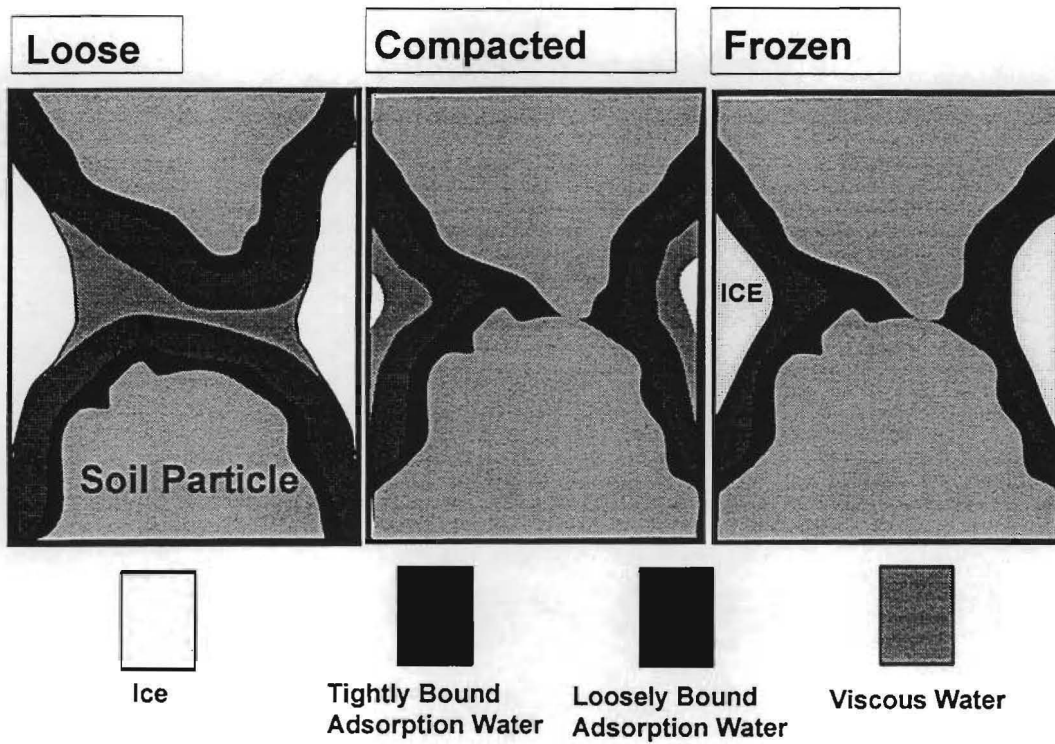


Figure 3. Adsorption Water in Loose, Compacted, and Frozen Micro Structures.

$$K^* = K' - iK''$$

where K' is the real part of the dielectric constant and K'' is the imaginary part or loss part of the dielectric constant (Davis and Annan 1989).

Imaginary part K'' can be also separated into high frequency components of loss in the form of

$$K^* = K' - i\left[K'' + \frac{\sigma_{dc}}{\omega \epsilon_0}\right]$$

where σ_{dc} is the dc conductivity (S/m), ω is the angular frequency, ($2\pi f$) and K'' is the frequency-dependent loss associated with relaxation response phenomena.

The real part of dielectric value can vary in nature between 1 (air) and 80 (free polar water at 20°C), but there are also some research results with dielectric values greater than 81 (Arulanandan et al. 1973, Campbell 1990, Knoll and Knight 1994). The dielectric value of water in soil depends on the degree of bonding of the water molecules around the soil particles so that the dielectric constant of tightly bound water close to the mineral surface is close to the dielectric constant of ice (3.5-3.8) (Dobson et al. 1985, Campbell 1990) even though the structure of water molecules is not the same. The dielectric value of most (oven) dry soil and aggregate solids varies between 4 and 6. Consequently the dielectric constant of soils gives information on both the volumetric water content of soil and also the amount of bound adsorption water. Sutinen (1992) found good correlation between clay content and dielectric constant for soils in Wisconsin. Dielectric dispersion, which is the change of real and imaginary parts of the dielectric constant with the frequency change, has also been found to be an important factor in some soils (Campbell 1990, Knoll and Knight 1994).

According to Knight and Knoll (1990) saturation hysteresis also affects the dielectric and conductivity values so that the dielectric value and electrical conductivity are higher during saturation than measured during the drying stage.

The electrical conductivity in soil is electron and ion movement with free or limited dislocations, which can be caused by different phenomenon. Most of the ionic or covalent bonded rock forming minerals, like quartz, different kinds of mica and feldspars, are nonconductors. When the surfaces of these minerals come in contact with liquid water, electrolytes are formed and ionic transmission generated by an external field causes electrical conduction. Ionic movement is proportional to electric field magnitude, and it is affected by temperature, ionic concentration and ionic size.

According to Mitchell (1992) dielectricity can affect both attractive and repulsive forces in the interparticle system in soils. Dielectric values affect both the surface potential and diffuse layer thickness. The energy of repulsion is sensitive to changes in electrolyte concentration, cation valence, dielectric value, and pH; whereas the attractive energy is sensitive only to changes in the dielectric value and temperature.

Coulomb's equation defines the classical relationship of the electrostatic attraction F between two charges Q and Q' separated by distance d (Mitchell 1992):

$$F = \frac{Q Q'}{K d^2},$$

where K is relative dielectric permittivity and d is distance between particles.

In other words in a highway base course at a certain temperature the attractive force between soil particles during the dynamic traffic load cycle when d is changing is dependent on the dielectric value of the water film between these particles. The tensile force is stronger the closer the particles are to each other and the lower the dielectric value. F decreases rapidly when free polar water molecules with dielectric value of 80 (or even higher) can penetrate between particles. This equation explains also the effect of compaction on the soil strength at low moisture contents.

2.4. GROUND PENETRATING RADAR AND OTHER TECHNIQUES IN MONITORING BASE MOISTURE CONTENT

GPR techniques are based on the measurement of travel time and reflection amplitude of a short electromagnetic pulse transmitted through a medium and then partly reflected from an electrical interface such as the base/subgrade interface. The two most important factors affecting the propagation of radar pulses in any material are the dielectric value and the electrical conductivity. The real part of the dielectric value affects the velocity of the signal in the medium and imaginary part, while electrical conductivity (ohmic conductivity) causes signal attenuation. The higher the real part of the dielectric, the slower the velocity of the radar wave in the material. The higher the imaginary part of the dielectric, the larger the signal attenuation within the material. As described earlier, the dielectric value of material is, in general, controlled by volumetric water content of the material while electrical conductivity in soils is mostly affected by temperature, ionic concentration and ionic size. Papers by Ulriksen (1982), Daniels et al. (1988), and Ground Penetrating Radar (1992) give more detailed descriptions of basic principles of GPR. A paper by Saarenketo and Scullion (1994) provides information on the use of GPR in road surveys.

GPR profiles measure the time that the GPR signal travels in layers. To transform time profile to a depth scale the dielectric value of material has to be estimated. Dielectric value in road surveys can be obtained by back calculating the signal velocity from reference data like drill cores or by different kinds of GPR sounding techniques, such as CDP (Common Depth Point) (Ulriksen 1982), WARR (Wide Angle Reflection and Refraction) (Annan et al. 1975) and GPR-RSAD technique (Sutinen and Hänninen 1990). The dielectric value of the road pavements can be calculated for a horn antenna by using the surface reflection technique (Maser and Scullion 1991), which is based on the reflection coefficient calculations at the asphalt/base interface (Figure 4). However when estimating the dielectric value of a base course, signal attenuation in the surfacing layer will cause errors in dielectric calculations. Little attenuation occurs in good quality asphaltic layers; however, greater attenuation may be observed in areas where de-icing salts are used or whenever the surface layer is concrete.

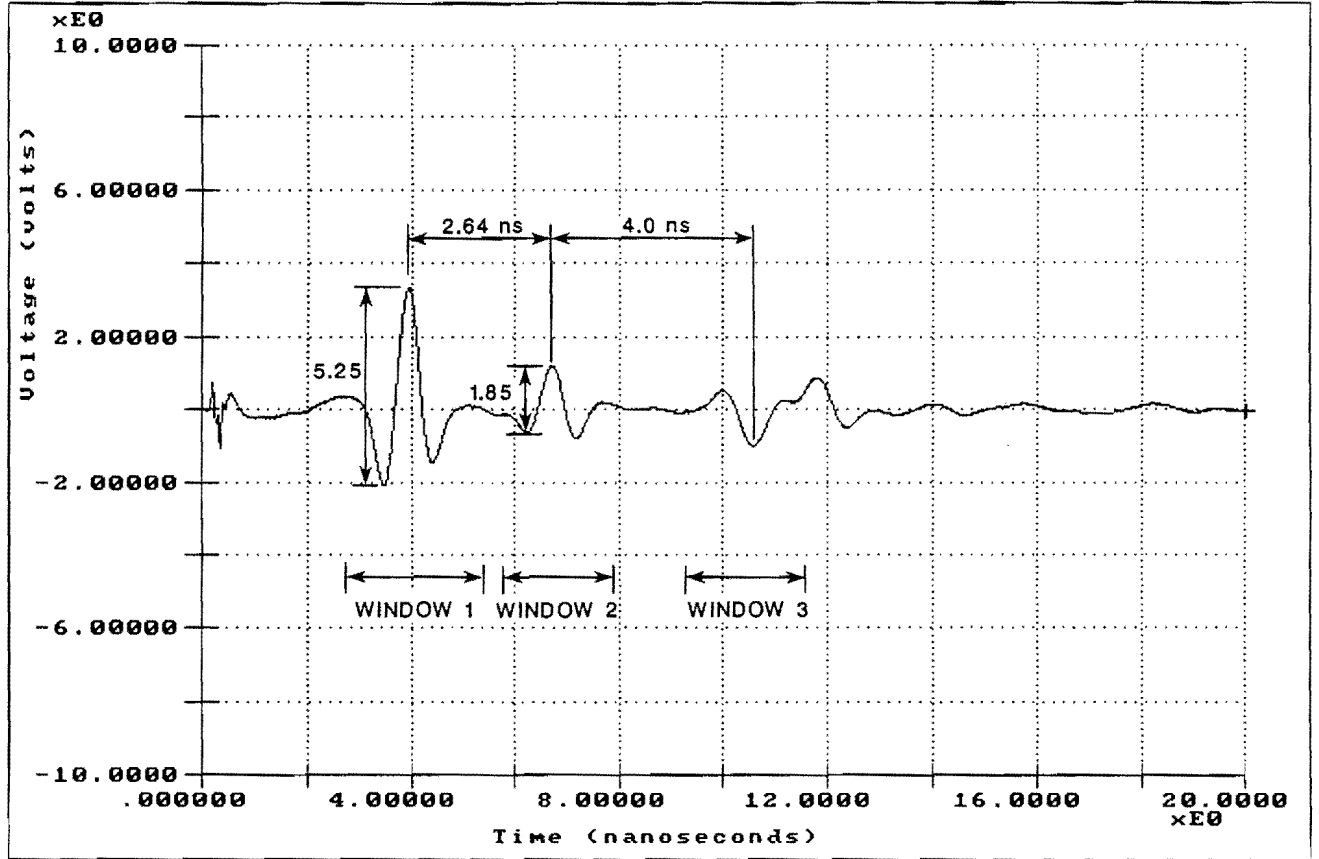


Figure 4. Calculating Layer Dielectrics Using the Surface Reflection Method. (Maser and Scullion, 1991).

The above GPR return is from an asphalt test block over a granular base. The amplitude of reflection from a large metal plate was 12.92 volts. The asphalt and base dielectrics are computed as follows:

$$\sqrt{\epsilon_{ac}} = \frac{A_m + A_0}{A_m - A_0} = \frac{12.92 + 5.25}{12.92 - 5.25} = 2.369$$

$$\sqrt{\epsilon_b} = \sqrt{\epsilon_a} \left[\frac{1 - \left[\frac{A_0}{A_M}\right]^2 + \left[\frac{A_1}{A_m}\right]}{1 - \left[\frac{A_0}{A_M}\right]^2 - \left[\frac{A_1}{A_m}\right]} \right] = 3.349$$

Dielectric properties can also be measured in the laboratory. As will be described in section 3.3 the capacitance dielectric probe measurement technique used in this study was based on the change of capacitance due to the influence of the material under test. The theory of this method has been described by Arulanandan et al. (1973), Mitchell (1992) and Plakk (1994). The central frequency of the probe is 50 MHz, which is relatively close to the GPR frequencies used in the field. The probe measures electrical conductivity with the inductance method with the 75 KHz central frequency (Plakk 1994).

The most advanced technique used in studies of pavement material electrical properties is Surface Network Analyzer technique which measures both the real and imaginary part of dielectric value through a wide range of GPR frequencies. The theory of this technique has been discussed by Lau (1991). The disadvantage of this technique is that it can be used only in laboratory, and successful measurements have been able to be made for only fine-grained materials.

Dielectric value of base course material can also be measured by Time Domain Reflectometry (TDR)-technique (Ravaska and Saarenketo 1993), and TDR-probes have been installed, for instance, in MINNROAD test sections in Minnesota and Elijahärvi test road in Finland. Radiometric moisture gauges have also been used for the base materials moisture measurements.

CHAPTER 3

MATERIALS AND STUDY METHODS

3.1. AGGREGATES, LITHOLOGY AND GRADING

Researchers selected the test materials for this research in cooperation with TxDOT to represent the typical base course aggregates used in Texas (samples 1-8). As reference material, three Finnish base aggregates (samples 14, 16, 17) were also tested. Six of the tested materials were crushed from bedrock, the remaining five from gravel. The lithology of the aggregates was visually analyzed. The names of the aggregates and their lithological composition are as follows:

#1. Limestone

- crushed rock aggregate consists 100 % of soft limestone;

#2. Granite / Basalt

- crushed rock aggregate consists of 69 % hard granite, 10 % loose and granular structured granite, 19 % hard diabase and 2 % loose and weathered diabase;

#3. Sandstone

- crushed rock aggregate consists of medium grained quartz rich sandstone, 68 % of which was light grey and 32 % yellowish in color;

#4. Dolomite

- crushed rock aggregate consists of 80 % grey and fine grained and 20 % yellowish and small grained hard dolomite;

#5. Iron Ore Gravel

- crushed river gravel consists of 71 % ovoidal iron ore fragments and 29 % looser granular fragments, both types were loose;

#6. Limestone

- crushed rock aggregate consists of 100 % limestone, which is harder than #1 Limestone;

#7. Caliche Gravel

- crushed river gravel consists of 71 % quartzite and sandstones, 21 % granitoid and 17 % limestone;

#8. Dolomite & Limestone Gravel

-crushed river gravel consists of 29 % hard dolomite, 68 % soft limestone and 3 % very soft limestone;

#14. Tohmo Granite

-crushed rock from Kemijärvi, Finnish Lapland, which consists of 100 % very hard medium grained granite. This aggregate presents a good quality crushed hard rock with extremely low water adsorption properties;

#15. Palovaara Gravel and #16. HW 955 Base

-crushed gravel base taken from HW 955 Kotakumpu-Nilivaara, Finnish Lapland, which is made of Palovaara glaciofluvial gravel (sample #15) consists of 24 % granitoid, 21 % quartzite, 16 % mica schists and phyllite, 24 % basic volcanites and 15 % greenstones and limestones. This extremely water sensitive and frost susceptible base aggregate (Saarenketo and Nieminen 1989) has been selected to present a known bad quality base aggregate; and

17. Hietavaara Gravel

-good quality crushed glaciofluvial gravel aggregate from Rovaniemi, Finnish Lapland, which consists of 39 % granitoid, 34 % quartzite, 4 % phyllite and 23 % diorite.

When processing the results, the test aggregates have been divided into three groups:

- a. Texas carbonate rocks (#1,#4,#6,#8),
- b. Other Texas aggregates (#2,#3,#5,#7), this groups includes also #7 Caliche

- Gravel even though it has carbonate rocks, and
- c. Finnish aggregates (#14,#15,#16,#17).

Grain size analysis results show that from the Texas aggregates, the carbonate hard rock aggregates (#1, #4 and #6) have the most "ideal" grading while #5 Iron Ore Gravel and #8 Dolomite & Limestone gravel had large amount of fine grained sand (see Appendix).

3.2. AGGREGATE FINES

The fine fraction grading of all the test aggregates were analyzed with a sedigraph in the Institute of Engineering Geology of the Tampere University of Technology in Finland. Figure 5 presents mass percentage curves of the aggregate fine fractions (<200 mesh).

The effect of wet sieving during the aggregate processing can be seen on the cumulative mass percentage curves of silt and clay fraction in Figure 5, where #1 Limestone has only coarser silt fractions in its fines. High amount of clay size particles (<0.002 mm) were found in samples #2 Granite/Basalt and #7 Caliche Gravel. Sample #5, Iron Ore Gravel, had more than 10% clay in the fine fraction.

The other fine fraction properties were studied by analyzing their mineralogy with X-ray diffraction, specific surface area by nitrogen adsorption method, density by helium pycnometer and water adsorption. Specific surface area, density and mineralogy of samples were analyzed in the Institute of Engineering Geology of the Tampere University of Technology in Finland, and cation exchange capacity (CEC) was measured by Soil Analytical Services, Inc. in College Station, TX.

The water adsorption was analyzed in TTI's laboratory at Texas A&M with a slightly modified method used in FinnRA. In this analysis about 1 g of fine fraction was dried in a china crucible in an oven at 105°C for 24 hours, and the oven dry samples were then weighed. After that the sample crucibles were placed in a closed exsiccator with water in the bottom and samples were again weighed every day until they reached equilibrium with the 100 % relative moisture content inside the exsiccator. Water adsorption was calculated as a percentage of increased weight from the sample dry weight. The measurement temperature was 21°C and changes in the air pressure were also taken into account in the calculations.

Grain Size Distribution of Aggregate Fines <0.074 mm

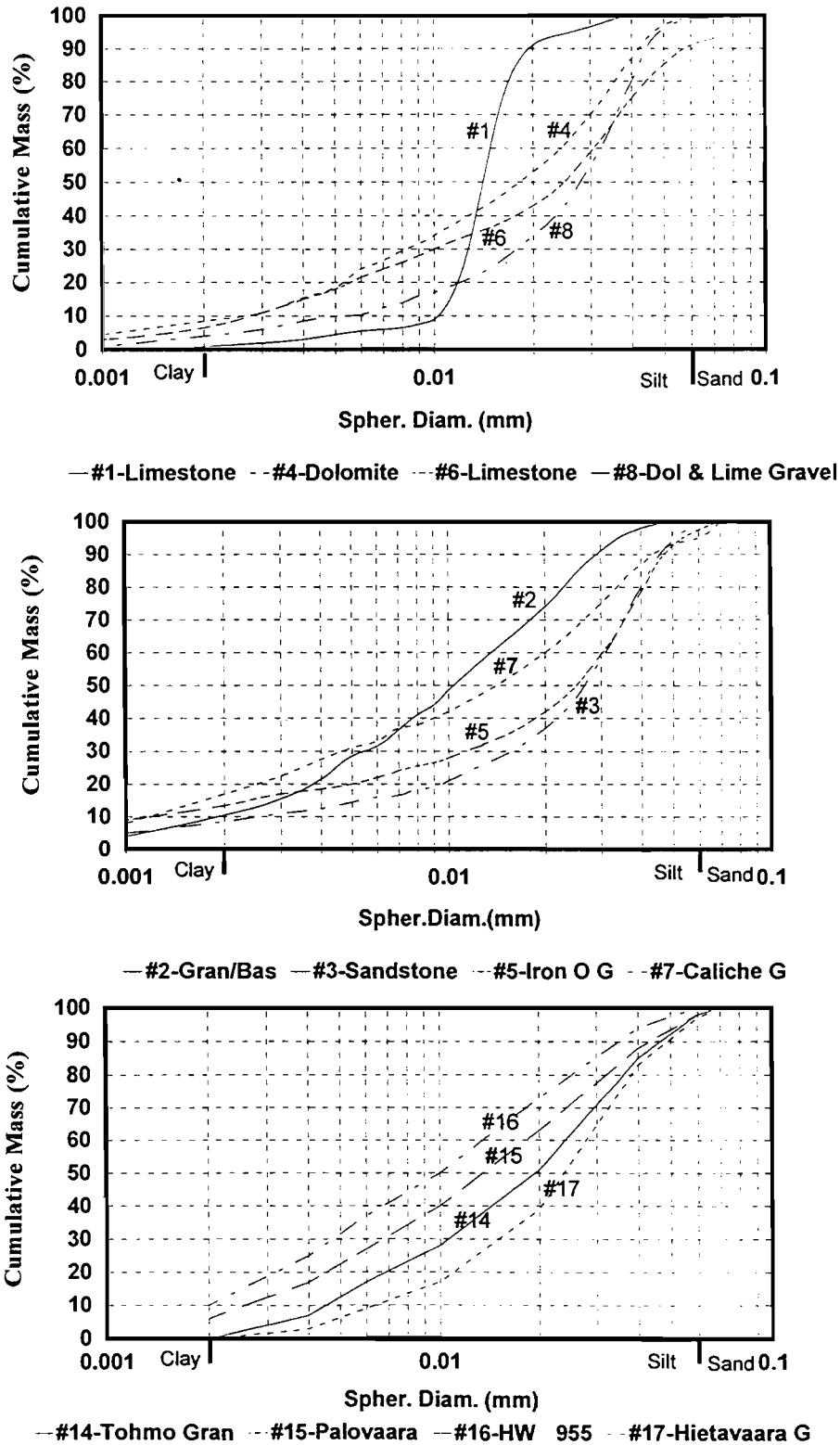


Figure 5. Grain Size Distribution of <0.074 mm (<200 mesh) Fraction of the Test Base Aggregates. Analysis was Made with Micromeritics Sedigraph.

Table 1 presents the summary of the test results. When comparing the specific surface area and water adsorption ratio with the previous survey results of Finnish aggregates (Figure 6), the Texas aggregate fines had much higher specific surface areas and water adsorption values. The implication of this high moisture adsorption will be discussed later in this text.

Table 1. Fine Fraction Properties of Test Materials.

| sample | density (g/cm ³) | spec. surface area (m ² /kg) | water ads. (%) | CEC (meg/100g) | main minerals | accessory minerals |
|-----------------------------|------------------------------|---|----------------|--------------------|---|-------------------------------|
| #1. Limestone | 3.11 | 6417 | 2.8 | 4.3 | CaCO ₃ , Quartz | |
| #2. Granite / basalt | 2.93 | 12 328 | 8.6 | 27.5 | Quartz, Plagioclase, Potassium feldspar | Chlorite |
| #3. Sandstone | 2.80 | 4670 | 2.2 | 3.7 | Quartz | |
| #4. Dolomite | 2.73 | 10 593 | 3.9 | 9.8 | Quartz, Potassium feldspar CaCO ₃ , CaMg(CO ₃) ₂ | |
| #5. Iron ore gravel | 2.96 | 12 851 | 6.6 | 6.9 | Quartz | Kaolinite |
| #6. Limestone | 2.66 | 6593 | 3.2 | 8.9 | CaCO ₃ , Quartz | |
| #7. Caliche gravel | 2.66 | 17 210 | 7.9 | 25.5 | CaCO ₃ , Quartz Plagioclase | Vermiculite |
| #8. Dolom. & Limest. gravel | 2.82 | 6530 | 2.3 | 4.3 | Quartz, CaCO ₃ , CaMg(CO ₃) ₂ | |
| # 14 Granite: Tohmoavaara | <i>no analysis</i> | 1700 | 0.6 | 4.3 | Quartz, Plagioclase, Muscovite, Hornblende | |
| #15 Palovaara Gravel | <i>no analysis</i> | 8390 | 3.2 | <i>no analysis</i> | Quartz, Talc, Chlorite, Plagioklase, Hornblende, | Biotite, Potassium feldsp. |
| #16 HW 955 Base | <i>no analysis</i> | 6260 | 3.0 | 8.2 | Quartz, Talc, Chlorite, Plagioklase, Hornblende | Biotite |
| #17 Hietavaara Gravel | <i>no analysis</i> | 2270 | 1.6 | 5.8 | Quartz, Plagioclase, Potassium feldspar, Muscovite, Hornblende | Muscovite |

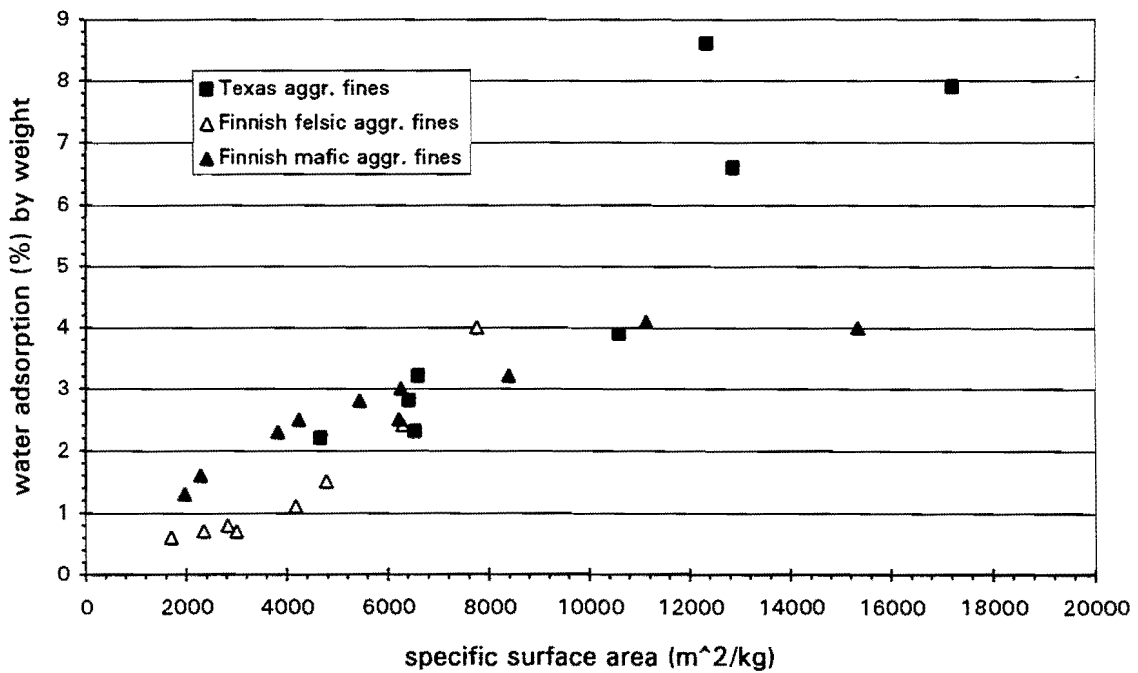


Figure 6. Comparison of Fine Fraction Properties of the Test Aggregates Together with the Finnish Base Course Materials Fine Fraction Study Results. The Finnish Materials have Classified as Felsic and Mafic Aggregates. Felsic Aggregates are Dominated with Granitoids and Mafic Aggregates have Higher Ferromagnesian Minerals Content.

The reason for the high specific surface area of the fine fraction was studied further. The main reason was thought to be the amount of clay particles in the fine fraction. Figure 7 shows that this is roughly true when discussing the large amount of clay particles in the fines. However, the correlation of the percentage of clay particles and specific surface area with the Finnish aggregate fines is not good, and the mineral surface properties, like surface porosity and roughness and hydrophobic - hydrophilic behavior of the fine materials, can be explained to be the reason for these changes.

The electrical properties of aggregate fines were also studied with the Surface Network Analyzer surface probe (Lau 1991). The real and imaginary part of the oven dry and water adsorbed fines were measured using surface probe with the frequency range of 30 MHz to 3 GHz (see Figures 12 and 13).

3.3. DIELECTRIC VALUE , ELECTRICAL CONDUCTIVITY MEASUREMENTS AND DCP- TESTS

Researchers used a special "bucket test" to obtain information on the dielectric value and electrical conductivity at different moisture contents and densities. This test had already been successfully used in Finland with Finnish aggregates (Marjeta 1993). In this test 40 kg of oven dry base course material < 18.8 mm (3/4 inch) is loosely placed in a 470 mm high and 285 mm diameter bucket. The volume of material was measured and the dielectric value and electrical conductivity were read from the middle of the sample using a tube probe and Dielectric and Electrical Conductivity Meter made by Adek Ltd in Estonia (Figure 8).

After the first measurement in the uncompacted condition, the material was lightly compacted by pressing the sample surface with a Proctor hammer and readings of the sample volume and dielectric were repeated. After the test the bucket was emptied and then filled again by compacting the material with a Proctor hammer in 50-60 mm layers with 40 blows/layer which equals the compaction force of the modified proctor test.

After compacting the sample and reading the sample volume, a DCP (Dynamic Cone Penetration) test was performed in the middle of the bucket. Finally, a dielectric probe measurement was taken in the DCP hole after widening the hole with a special steel spike.

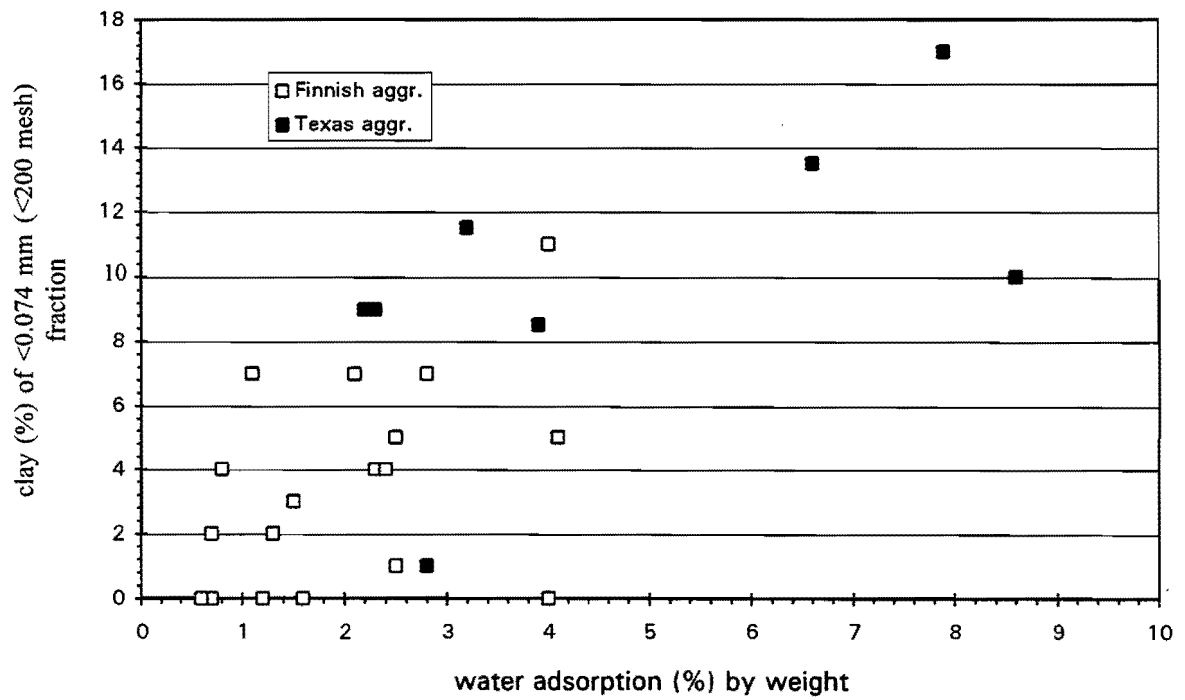


Figure 7. Correlation Between Water Adsorption and Clay Content in the Fine Fraction of the Test Aggregates.



Figure 8. Dielectric Tube Probe of Dielectric and Electrical Conductivity Meter, Proctor Hammer and Test Bucket Used in the Test.

This test was repeated on the same base material with increasing moisture content (2, 4, 6, 8, 10, 12 %) or until the material had become so plastic that the DCP test could not be performed. Measurements were also terminated when materials could not hold the additional water which filtrated to the bottom of the bucket. However, this happened only with the Finnish aggregates #14 Tohmo Granite and #17 Hietavaara gravel. A concrete mixer performed material mixing, and the mixing time was kept constant at 5 min.

In order to study the effect of wetting and drying hysteresis on the dielectric and strength properties a special drying test was performed. After the last test the material was again compacted into the bucket, and the bucket was placed in a drying room for a period of about one week. After that, the DCP-test was repeated and dielectric value and electrical conductivity were measured at different depths. The calculated California Bearing Ratios (CBR) were compared at each depth with dielectric properties from the same depth.

The results of the DCP-test were transformed to CBR values with the equation developed by US Army Corps of Engineers (Webster et al. 1992).

3.4. RESILIENT MODULUS TESTS

The resilient moduli of some selected samples were measured in cooperation with the researchers of the Super Heavy Load Project in TTI (Titus-Glover and Fernando 1995). This test was performed with only four test aggregates (samples #2, #8, #14 and #16) at two moisture contents. The test method slightly differed from Super Heavy Load Project tests in that all the samples were molded at same moisture content and then another sample was allowed to dry in environmental room at about 45°C temperature for two days. After that the dried sample was removed from the high temperature room and left for one day to attain room temperature. In this way both the moist and dried samples were tested at the same dry density, and information of the saturation hysteresis were able to be gained.

Resilient properties of these aggregate bases were measured in a conventional triaxial cell arrangement using the procedure developed from the Strategic Highway Research Program A005 project and using AASHTO T-274 as a guide. The sample size was 152 mm diameter by 305 mm height. Both radial and vertical strains were measured via Linear Variable Differential Transformers (LVDT's) clamped to the sample.

The procedure for measuring the resilient properties was as follows:

- a. The specimen was prepared and molded using a metal cylinder 305 mm high and 152 mm in diameter. It was then extruded and placed in a rubber membrane as recommended by AASHTO.
- b. To condition the specimen, 200 repetitions of a square wave were initially applied to the test specimen. The specimen was loaded for 0.1 seconds and then allowed to recover for 0.9 seconds. This was done starting at the highest confining pressure and then at subsequent confining pressures.
- c. After conditioning, a single load and unload cycle was applied to the specimen using a prescribed deviatoric stress. This was in the form of a square wave load pulse applied for 90 seconds after which the specimen was unloaded and allowed to recover.
- d. The confining pressure was reduced to the next prescribed level and steps (b) and (c) repeated until the final and lowest confining pressure was run. Note that AASHTO T-274 was used as a guide in conducting this test.
- e. Three LVDT's were used for measuring axial deformation and three LVDT's were used to measure the radial deformation. In both cases, these were placed 120° apart and a 130 mm gauge length centered along the height of the cylindrical mold was used to measure vertical and radial displacements.
- f. The strains (vertical and radial) and the applied load were used to obtain vertical and radial compliance curves.

Researchers used the compliance equations to obtain the resilient strains at specified loading times and stress states. Researchers used the results to calculate the K_1 , K_2 , and K_3 terms from the equation below. This is the universal resilient modulus equation proposed by Uzan (1985).

$$E = K_1 P_a \left(\frac{I_1}{P_a} \right)^{K_2} \left(\frac{\tau_{oct}}{P_a} \right)^{K_3}$$

where

- E = resilient modulus;
- P_a = atmospheric pressure;
- I_1 = first stress invariant (1+2+3 with i = stress);
- τ_{oct} = octahedral shear stress; and
- K_i = material constants.

This universal material model simplifies in certain instances. In granular materials, for example, K_3 is set to zero. The equation above thus reduces to

$$E = K_1 P_a \left(\frac{I_1}{P_a} \right)^{K_2}$$

As the material changes from granular to fine grained, the K_2 value approaches zero. The model is flexible and is capable of a resilient modulus decrease as the octahedral shear stress increases and a resilient modulus increases as the first stress invariant increases. These phenomena are observed in practice. It also represents the stiffening effect observed in laboratory tests that results in an increase of resilient modulus as both the first stress invariant and the octahedral shear stress increase at large deviatoric stresses or large octahedral shear stresses. This stiffening effect is believed to be a characteristic of a granular material in a dense state and is related to the dilation phenomenon in granular materials.

Before each of these resilient modulus tests the dielectric value and electrical conductivity were also measured with the Dielectric and Electric Conductivity Meter surface probe at four places from the sample surface and bottom. The highest and lowest measured value was ignored, and final result was the mean value of the middle two measurement results.

3.5. TUBE SUCTION TESTS

To estimate what is the equilibrium level of moisture in the base course, if water was available, researchers developed a special "tube suction test". In this test base aggregates (19 mm maximum size) were compacted at optimum Proctor moisture content into a 305 mm high

and 152 mm diameter plastic tube, which had 1 mm diameter holes about 10 mm above the bottom. Researchers dried the compacted samples for 10 days at a temperature of about 50°C. After drying, the dielectric value and the electrical conductivity of the dry material were measured on the sample surface with Dielectric Constant and Conductivity Meter surface probe. Dielectric value and electrical conductivity were calculated with the method described in section 3.4. The samples were also weighed.

The dried aggregate samples were then placed in a plastic tank with 20 mm of deionized water (Figure 9). The water suction of the aggregate samples was measured by monitoring the changes in surface dielectric value over time. Sample weight was also recorded until the sample reached equilibrium. After that, the water level was increased in 20 mm intervals between 280 and 60 mm from surface and from depth of 60 mm to the surface with 10 mm intervals. After each increase in water level, the dielectric value and electrical conductivity were measured from the sample surface after 2 days, and the increasing of water content was estimated by weighing the sample. The test was terminated when the sample was totally saturated with water. After that the samples were dried in an oven in order to get their dry weight.

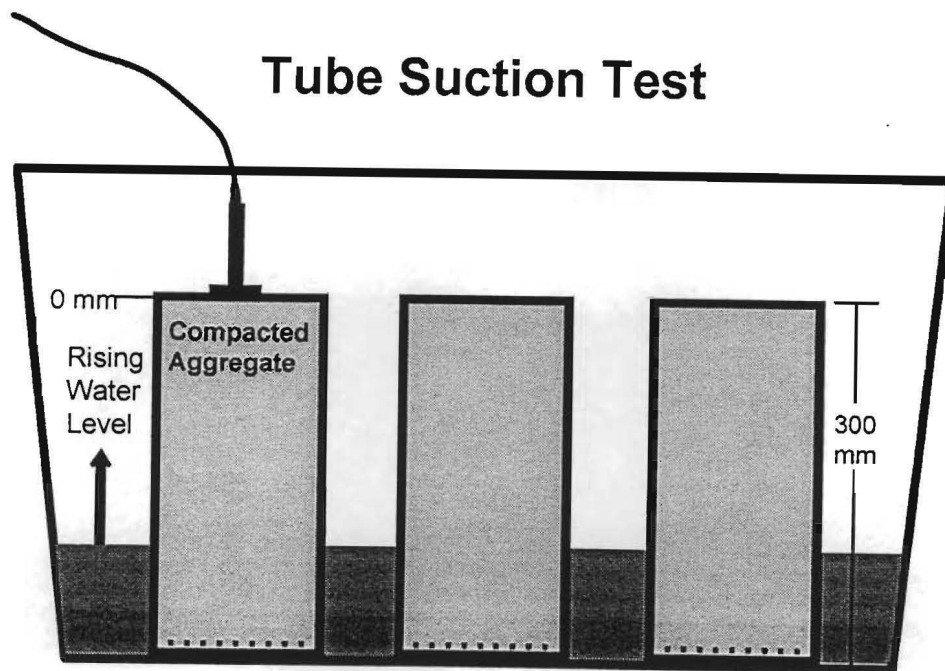


Figure 9. Tube Suction Test Arrangements.

3.6. FREEZING TEST

To evaluate what range of dielectric values should be expected if GPR surveys were performed in winter when the base course is frozen and what the effect of freezing and thawing is on these materials, a test was arranged to simulate freeze/thaw cycle in road bases. This freezing test was performed with the same samples as those used in the suction tests described in section 3.5.

In the first phase, the test samples were allowed to reach moisture equilibrium in a plastic tank with the water level of -270 mm (=30 mm water in the bottom of tank). After measuring the dielectric value and electrical conductivity and weighing the sample the tank was moved into an environmental room with the temperature of -5°C. To prevent the water from freezing too fast, a 50 mm polystyrene plate insulated the water surface, which reduced the rate of freezing. The water did not become frozen for 20 to 25 hours after placing the sample in the cold room.

Dielectric value and electrical conductivity were measured from the sample surface after 24 hours, one week and two weeks. Samples were weighed and allowed to thaw after two weeks period. The dielectric value of the thawed aggregate was measured 24 hours after the samples were taken from the environmental chamber.

CHAPTER 4

RESULTS AND DISCUSSION

4.1. PREVIOUS SURVEYS WITH FINNISH AGGREGATES

The first "bucket" tests on several different kinds of Finnish aggregates were performed in 1993 together with a study to determine if dielectric probe measurement technique could be applied to measuring the moisture content of cold mix pavement aggregate stock piles (Marjeta 1993). In these tests known problematic aggregates, which were water sensitive and exhibited poor performance during the frost thawing in spring, were compared with good performers. The dielectric values of the problem aggregates were much higher at the same gravimetric water contents (Figure 10). Mafic aggregates also had higher dielectric value when comparing the values with the volumetric water content. For example, at water content of 12 % by volume, the dielectric value of mafic aggregates vary between 12 and 14; the corresponding value for felsic aggregates is around 10.

Another observation was that the degree of compaction seemed to affect the dielectric value at the low moisture contents in "good quality" aggregates. This can be explained by reducing the volumetric amount of bound adsorption water with low dielectric value by the compaction (see also Figure 3). However, with problem aggregates the effect of compaction on the dielectric value vs. volumetric moisture content could be seen through the whole moisture range (Figure 11).

4.2. ELECTRICAL PROPERTIES OF AGGREGATE FINES

Table 2 presents the summary of the Surface Network Analyzer test results. In this table the K' - (real) and K'' - (imaginary part) values of dry aggregates have been subtracted from water adsorbed values in order to eliminate the effect of mineralogy on the dielectric properties of adsorption water.

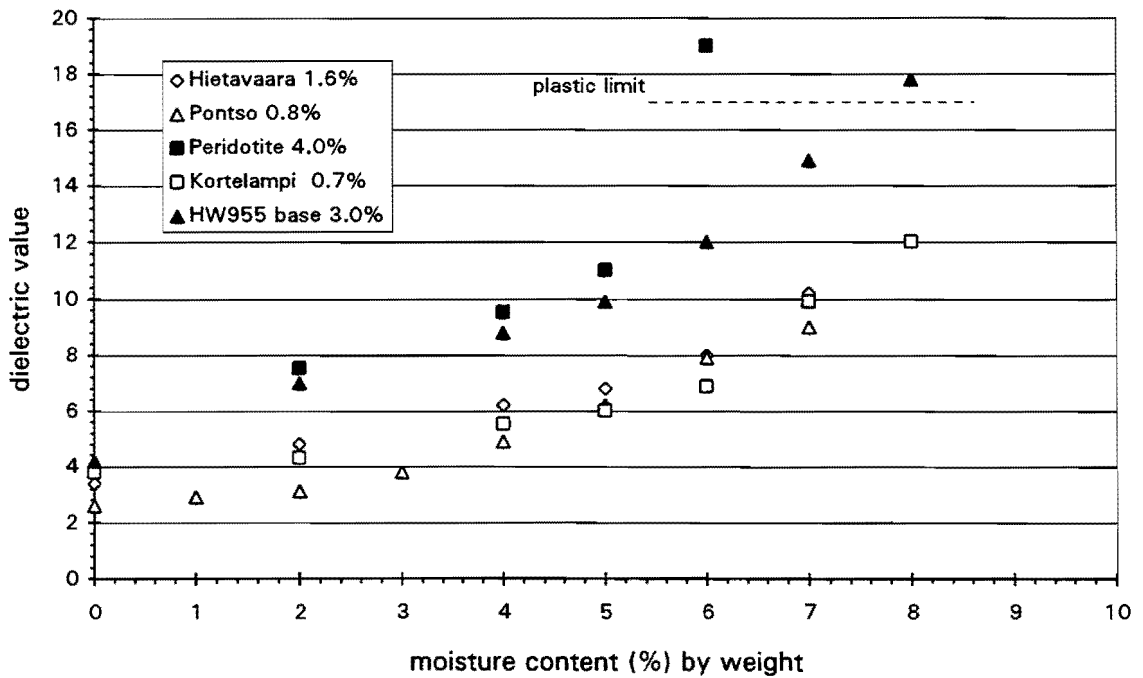
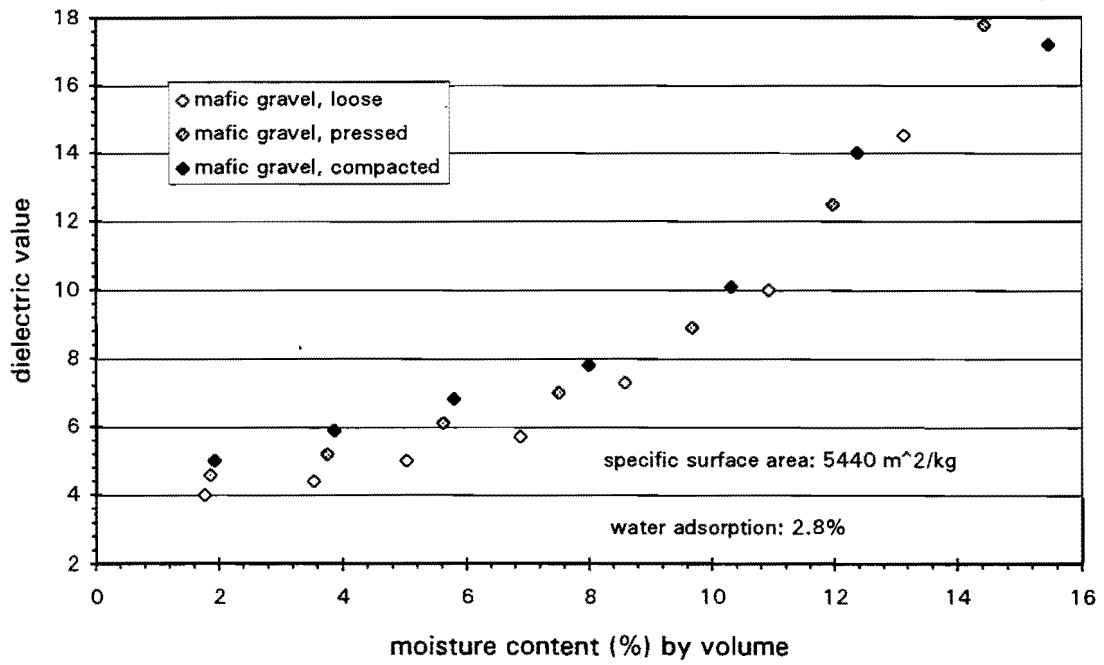
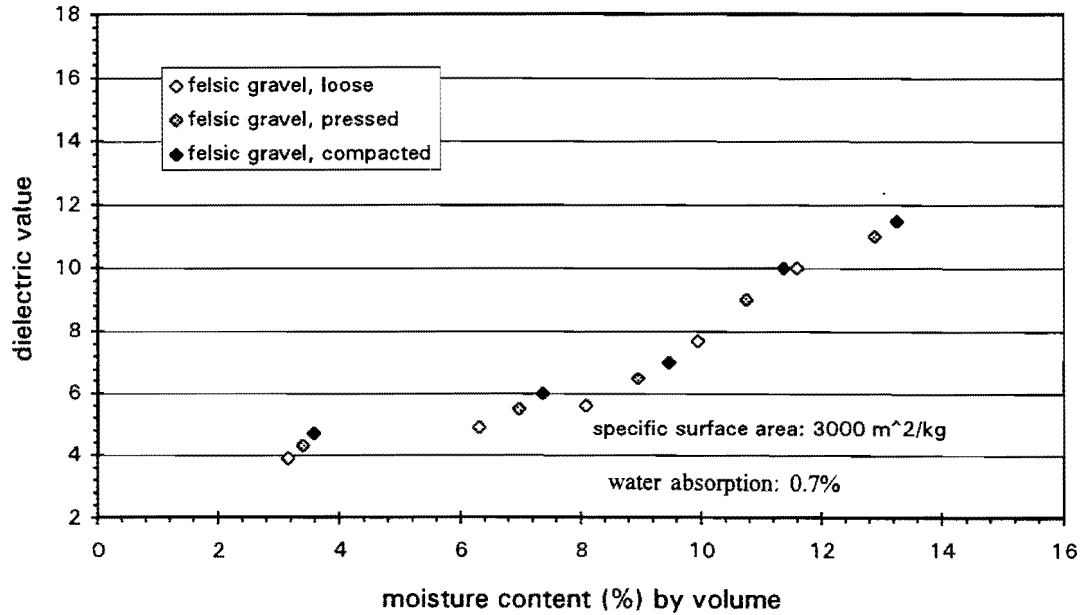


Figure 10. Dielectric Value at Different Gravimetric Moisture Contents of Finnish Aggregates. Filled Square and Triangle Represent Moisture Sensitive Aggregates with High Water Adsorption Values, which are Presented after Aggregate Names.



(a) Bad Performer



(b) Good Performer

Figure 11. Correlation of Dielectric Value and Volumetric Water Content of Two Types of Finnish Base Aggregates.

Table 2. Real and Imaginary Part of the Dielectric for the Study Aggregates After Water Adsorption. (the dry aggregate value has being subtracted)

| Aggregate | K' - 0.12 GHz | K' - 0.5 GHz | K' - 1.0 GHz | K' - 3.0 GHz | K''' - 0.12 GHz | K''' - 0.5 GHz | K''' - 1.0 GHz | K''' - 3.0 GHz |
|-----------------------|---------------------|--------------------|--------------------|--------------------|-----------------------|----------------------|----------------------|----------------------|
| #1 Limestone | 2.2 | 1.5 | 1.4 | 1.3 | 0.4 | 0.3 | 0.3 | 0.2 |
| #2 Granite/Basalt | 9.5 | 5.4 | 4.7 | 4 | 10.1 | 3.2 | 2.1 | 1 |
| #3 Sandstone | 4.7 | 2.7 | 2.5 | 2.2 | 4 | 1.3 | 0.8 | 0.4 |
| #5 Iron Ore Gravel | 2.9 | 2.1 | 1.9 | 1.8 | 1.5 | 0.5 | 0.3 | 0.2 |
| #6 Limestone | 4.4 | 2.5 | 2.1 | 1.9 | 5.9 | 1.8 | 1.1 | 0.5 |
| #7 Caliche Gravel | 6.5 | 4.7 | 3.9 | 3.3 | 11.7 | 4 | 2.4 | 1 |
| #8 Dol. & Lim. Gravel | 2.6 | 1.5 | 1.2 | 1 | 3.9 | 1.4 | 0.6 | 0.2 |
| #14 Tohmo Granite | 0.9 | 0.4 | 0.3 | 0.3 | 0.9 | 0.4 | 0.1 | 0 |
| #16 HW 955 Base | 2.5 | 1.2 | 1 | 0.7 | 3.2 | 1 | 0.4 | 0.2 |
| #17 Hietavaara Gravel | 1.3 | 0.6 | 0.6 | 0.4 | 1.2 | 0.4 | 0.2 | 0.1 |

Table 2 shows that high components of the dielectric (K') at low GPR frequencies were measured for sample #2 Granite/Basalt fines, and the highest K''' -values were measured on Caliche gravel. Lowest adsorption water K' and K''' - values were measured from Tohmo granite fines. Wet sieving of the sample #1 Limestone also has a large effect on K' and K''' - values, which are much smaller than those measured on other carbonate aggregate fines.

Figures 12 and 13 provide a graphic representation of the real and imaginary parts of the dielectric value of dry and water adsorbed fines at different GPR frequencies, and results of three different types of aggregate fines (see Table 1) are compared. The aggregates compared in these figures are Tohmo granite with very low water adsorption value (0.6 %), limestone with medium water adsorption value (3.2 %), and granite/basalt fines with extremely high water adsorption value (10.0 %).

The real parts K' of all oven dry aggregate fines vary between 2 and 4 and they are not frequency dependent, but the values vary markedly when comparing the water adsorbed results (Figure 12). The real part of Tohmo granite fines is very low and it is only slightly frequency dependent, whereas limestone and granite/ basalt fines have much higher K' -values and they are

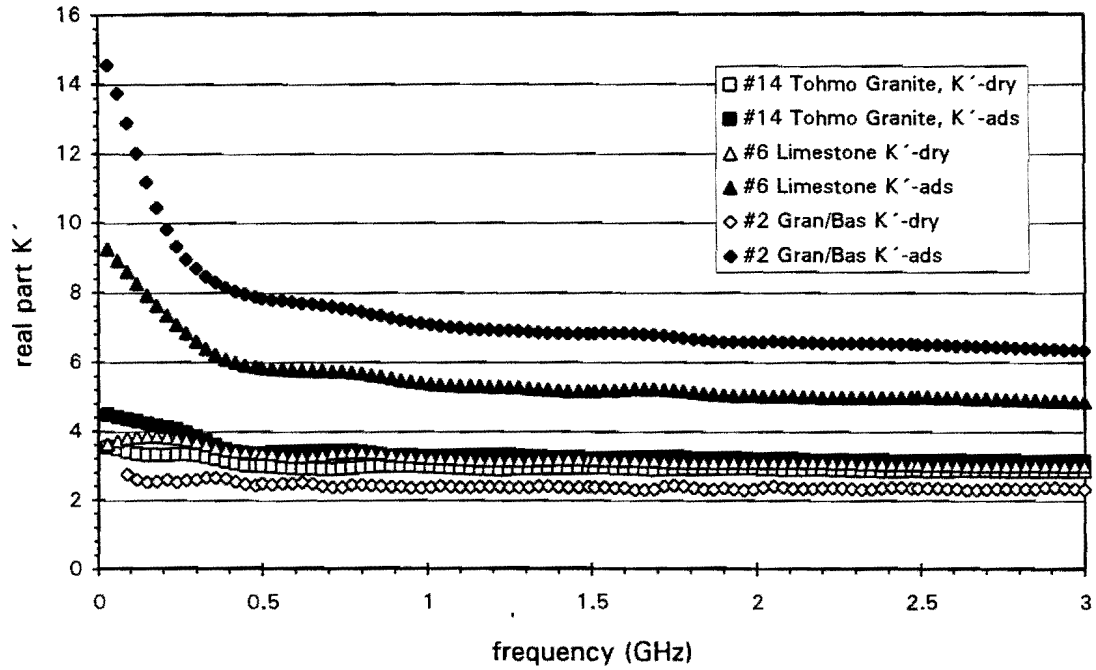


Figure 12. Real Part (K') of Dielectric Value of Three Different Types of Aggregate Base Fines between the measurement frequencies of 30 MHz and 3 GHz. Measurements with Surface Network Analyzer Surface Probe Have Been Made from Oven Dry Samples and Samples Balanced with 100 % Relative Air Moisture at Room Temperature.

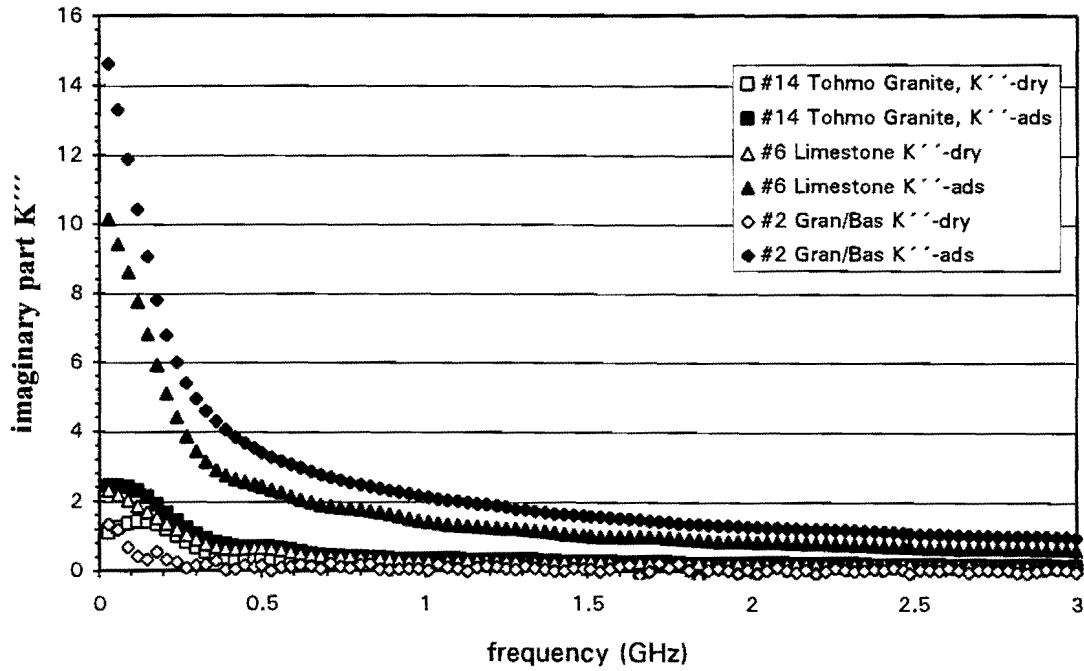


Figure 13. Imaginary Part (K'') of Dielectric Value of Three Different Types of Aggregate Base Fines between the measurement frequencies of 30 MHz and 3 GHz. Measurements with Surface Network Analyzer Surface Probe Have Been Made from Oven Dry Samples and Samples Balanced with 100 % Relative Air Moisture at Room Temperature.

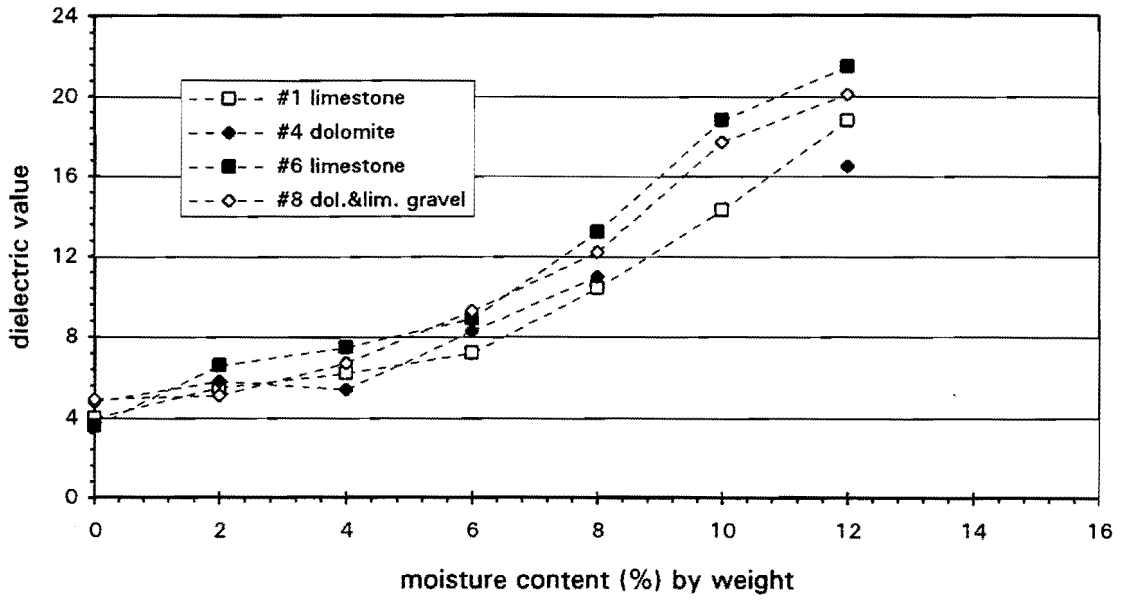
very dispersive at GPR frequencies lower than 0.4 GHz. Another noticeable but smaller step of K' is around 1.0 GHz. The dielectric dispersion of K' seems to correlate well with the water adsorption values and CEC presented in Table 1.

Imaginary part values K'' of all oven dry aggregates are close to 0 at higher GPR frequencies and are slightly higher at lower frequencies (Figure 13). Also the imaginary part of water adsorbed Tohmo granite fines is insignificant at higher frequencies. However K'' -values of #6 limestone and #2 granite/basalt fines are so high at GPR frequencies lower than 0.5 GHz, that it will have an effect on the GPR signal attenuation even when dry base materials are tested with GPR.

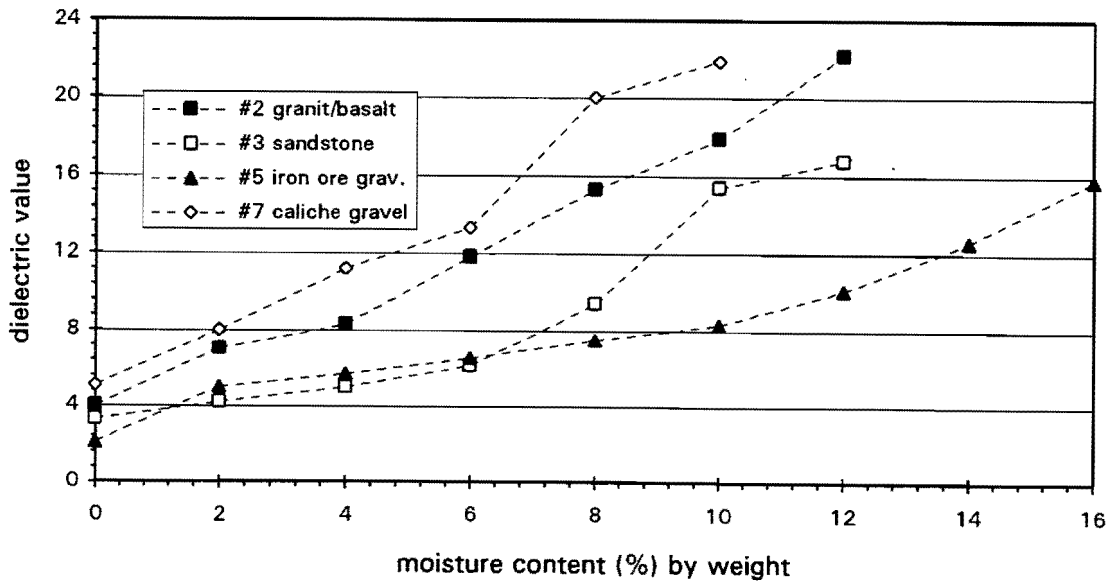
4.3. RELATION BETWEEN DIELECTRIC VALUE AND ELECTRICAL CONDUCTIVITY AND MOISTURE CONTENT

Figure 14 presents results of the dielectric values vs. gravimetric moisture content of compacted Texas aggregates, and Figure 15 illustrates the electrical conductivity vs. gravimetric moisture content. All the carbonate aggregates have similar dielectric value versus gravimetric water content relationships, and similar results were observed when comparing electrical conductivity and gravimetric water content. Sample #3, Sandstone, also had similar behavior. However the dielectric distribution of samples #2, #5 and #7 varied markedly. Samples #2 and #7 had similar high dielectric value/moisture content ratios to the mafic type problem aggregates in Finland (see Figure 11). Sample #5, Iron Ore Gravel, had low dielectric value/moisture content ratio and behaved as the mica rich problem aggregates in Finland which adsorb considerable water but their dielectric value remains low.

A similar trend can also be seen when analyzing the electrical conductivity - gravimetric moisture content data in Figure 15. Electrical conductivities of Texas carbonate aggregates do not start to increase until the moisture content passes the adsorption water phase. On the other hand samples #2 and #7, with high CEC, have almost a linear correlation with moisture content. Results also show that #5 Iron Ore Gravel can have over 10 % tightly bound water before free water starts to appear.

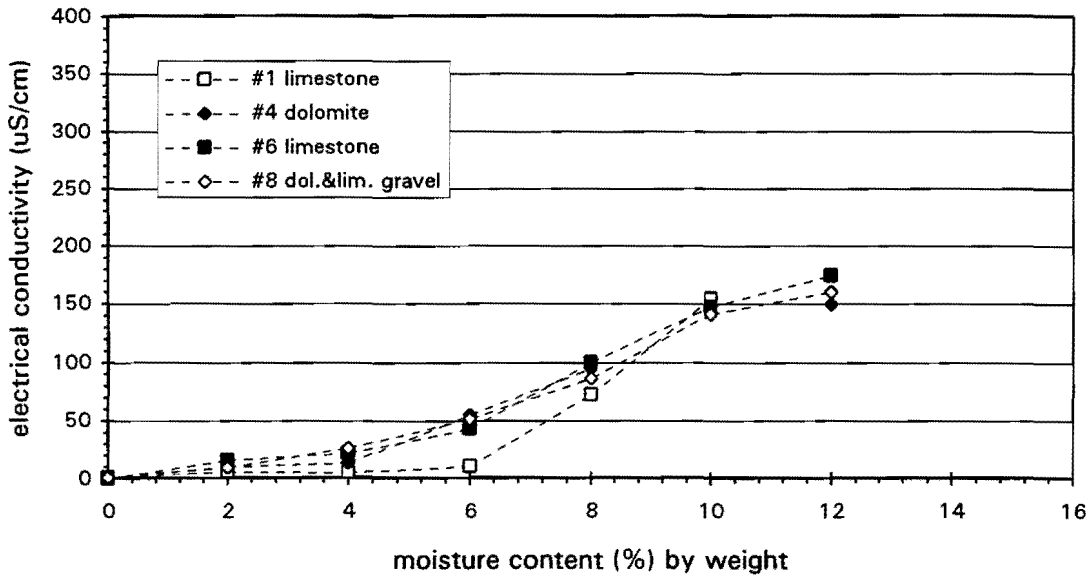


(a) Texas Carbonate Aggregates

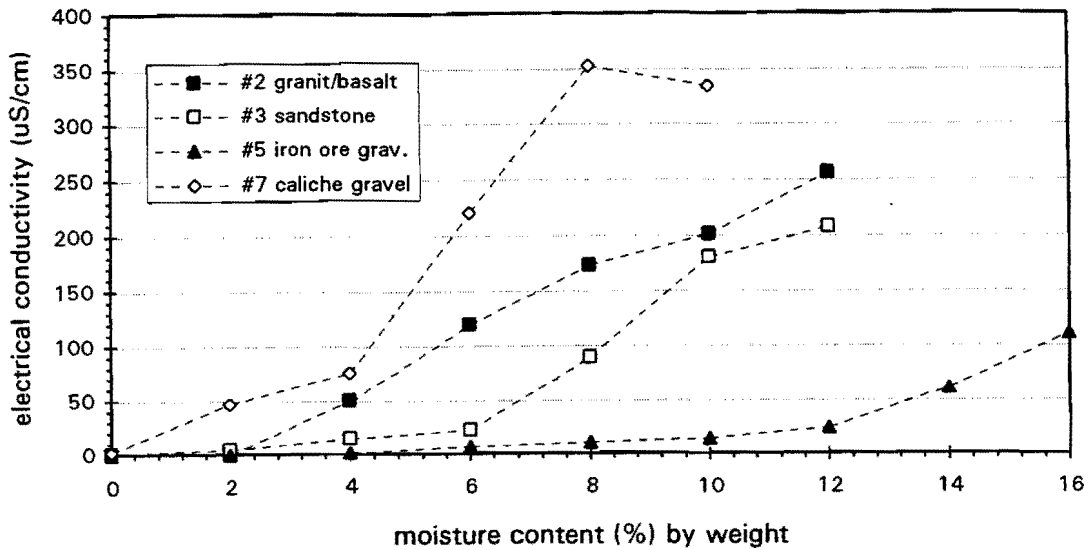


(b) Other Texas Aggregates

Figure 14. Correlation Between Dielectric Value and Gravimetric Moisture Content of Texas Aggregates.



(a) Texas Carbonate Aggregates



(b) Other Texas Aggregates

Figure 15. Correlation Between Electrical Conductivity and Gravimetric Moisture Content of Texas Aggregates.

4.4. COMPACTION DEGREE, DEGRADATION AND SOLUBILITY

The dry density of the uncompacted and compacted aggregates was also recorded during the bucket tests. Figures 16 and 17 present the moisture density curves of aggregates with different electrical properties.

The effect of the water adsorption on the repulsive forces in the aggregates can be clearly seen in Figure 16, where the dry densities of selected uncompacted test aggregates are presented as a function of gravimetric water content. Dry densities of all oven dry aggregates varied between 1.6 and 1.7 g/cm³, but when moisture was introduced to the aggregates the dry densities of the uncompacted aggregates were reduced. The loosest structure (1.3 g/cm³) was measured with #2 Granite/Basalt and #7 Caliche gravel, which had the highest water adsorption values.

The compaction moisture density curves of most of the aggregates were different from those expected because they did not follow the standard moisture - density distribution. The maximum (Proctor) dry density of base materials should have been in the moisture range of 5 - 9 %. The reason for this is probably the effective disintegration of the aggregates during the water mixing and compaction cycles, which produced more fines, and, as described earlier, increased the amount of adsorption water and repulsive forces against compaction effort. At the higher water contents, these forces turn to the attractive forces, and very high dry densities can be achieved with relatively low compaction efforts. For example, at moisture content of 12 % the dry density of uncompacted samples #2, #3 and #6 is higher or about the same as the dry densities of the same materials compacted at the moisture contents of 0 to 4 %. This disintegration process simulates the kind of deterioration that occurs in the top part of unbound base material during the road construction, which makes the material more sensitive to water.

The amount of disintegration of the test aggregates, the grain size distribution, was also analyzed after the compaction test. Figure 18 shows the increase of fine fraction percentage. The greatest increase of fines happened with #1 limestone (14.4%) and #7 caliche gravel (10.6%), while #3 sandstone produced only 2.6% more fines during this test.

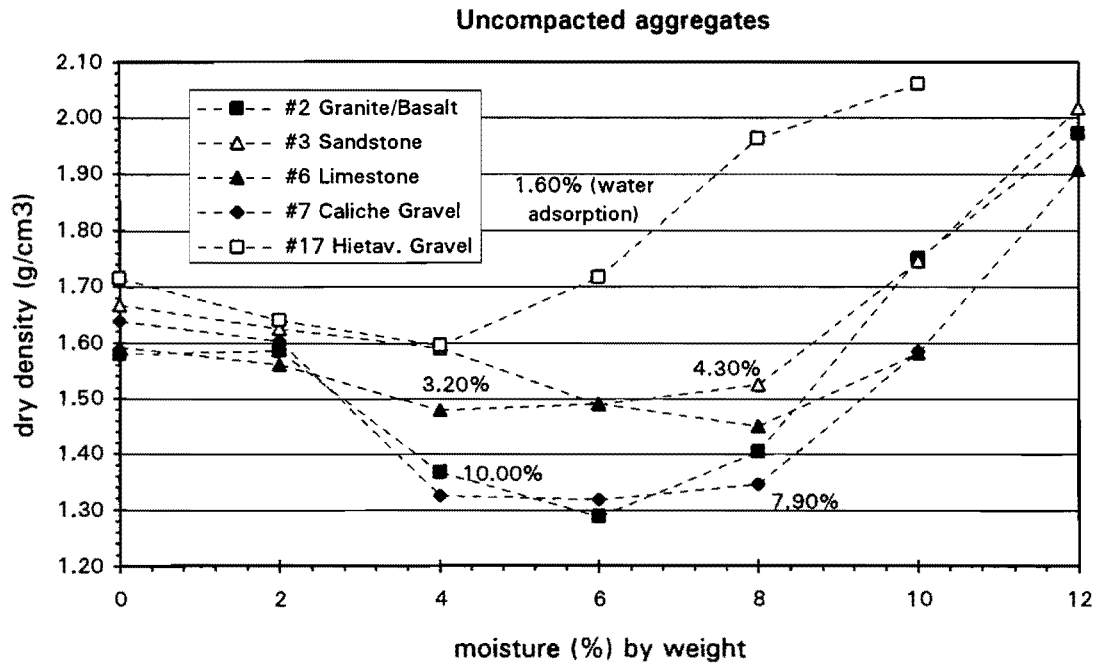


Figure 16. Moisture vs. Dry Density Relation of Different Types of Uncompacted Test Aggregates. Water Adsorption Values are Also Marked to Each Moisture-Density Curve.

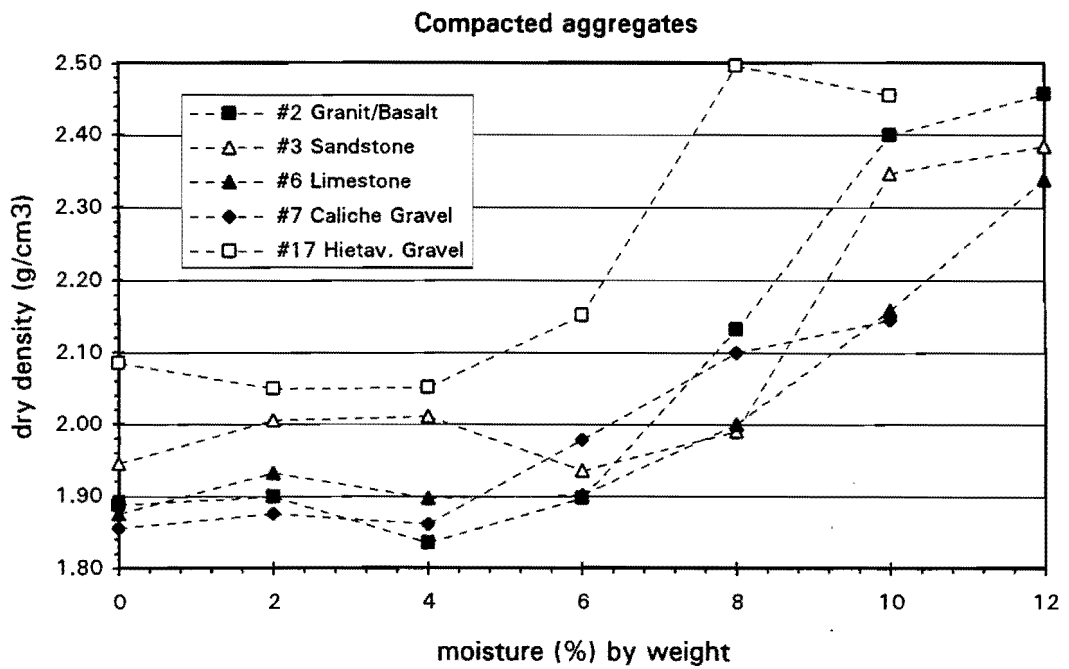


Figure 17. Moisture vs. Dry Density Relation of the Compacted Aggregates Presented in Figure 16.

Increase of Fines During the Compaction Test

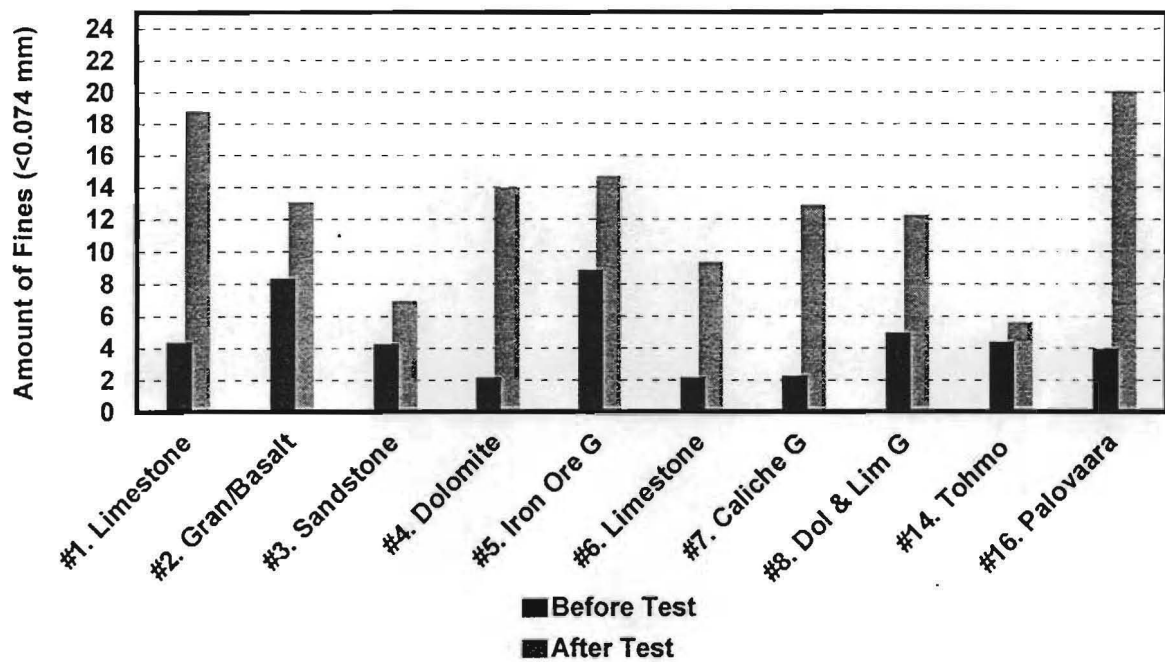


Figure 18. The Increase of Fines of Test Aggregates During the Compaction Test.

Part of the fine minerals such as calcium carbonate or dolomite may also dissolve into water, or hydrolytic reactions have formed minerals with water in crystalline structure. The evidence of these phenomena could be found when comparing the calculated and analyzed water contents at different moisture contents. For example, the calculated and, afterwards, analyzed water contents with #6. limestone were 4 / 3.8 %, 8 / 7.2 % and 12 / 9.1 %. These reactions happen especially with higher moisture contents, and this can cause errors in some aggregates when calculating volumetric water content or saturation level.

4.5. DCP- AND RESILIENT MODULUS TESTS

Figures 19, 20 and 21 present the relationship of the mean CBR-value calculated from DCP-test results and the gravimetric water content, dielectric value and electrical conductivity. The correlation of the CBR-value to the gravimetric moisture content (Figure 19) was poor, especially in the moisture range of 6% to 12%, which shows that gravimetric water content does not adequately explain the changes in strength properties when considering all the aggregates.

When comparing CBR-value to dielectric value (Figure 20) the correlation is better. However the correlation was not similar for each aggregate. From a review of these data the aggregates were divided into three group according to their behavior:

- a. CBR-values decrease almost linearly with the increasing dielectric value. This was the case especially with the samples #2, #3, #5, #7 and #16.
- b. CBR-values decrease in low dielectric values, but then stay constant until after a dielectric value of 16. The values then dramatically drop as the material turns to plastic. This type of behavior occurred with all of the Texas carbonate aggregates, excluding #8, which had a higher CBR-value than the other aggregates at higher moisture contents before loosing its strength when dielectric value became higher than 16. Dielectric - strength distribution curves of these materials were very similar to the moisture - suction curves presented in Figure 1.

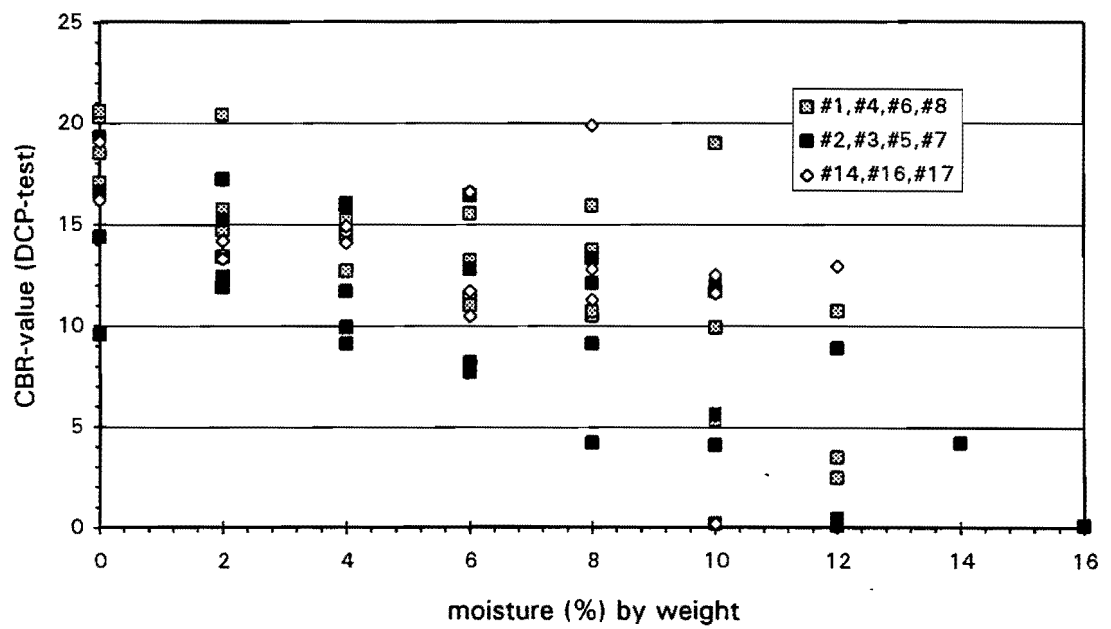


Figure 19. Correlation Between CBR-Value and Gravimetric Moisture Content of the Test Aggregates. Grey Squares Present Texas Carbonate Aggregates, Black Squares Other Texas Aggregates and Open Diamonds Finnish Aggregates.

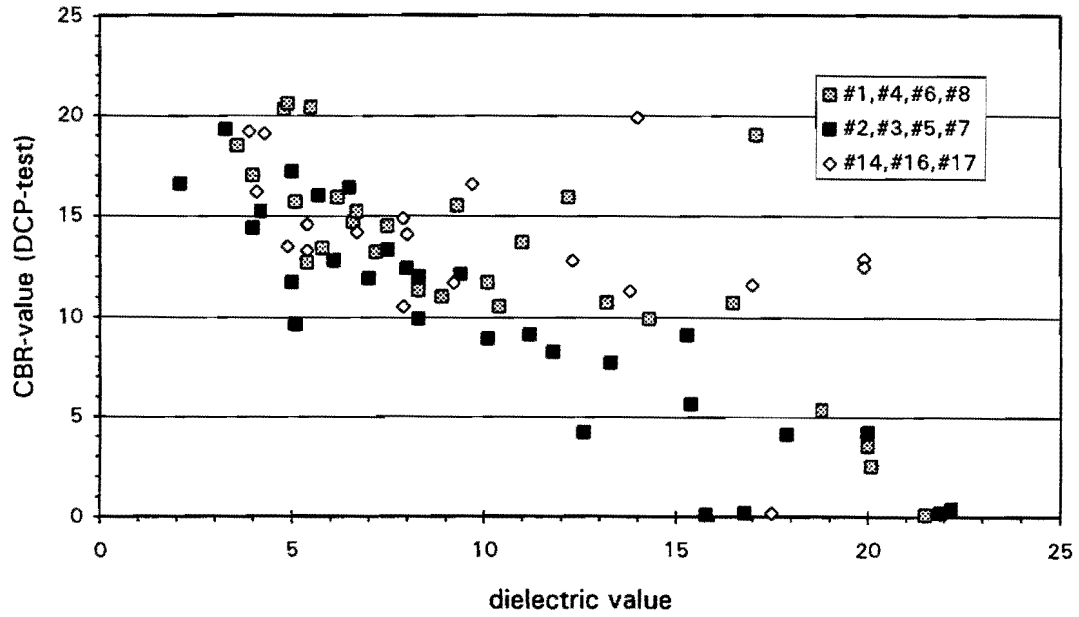


Figure 20. Correlation Between CBR-Value and Dielectric Value of Texas and Finnish Test Aggregates. Grey Squares Present Texas Carbonate Aggregates, Black Squares Other Texas Aggregates and Open Diamonds Finnish Aggregates.

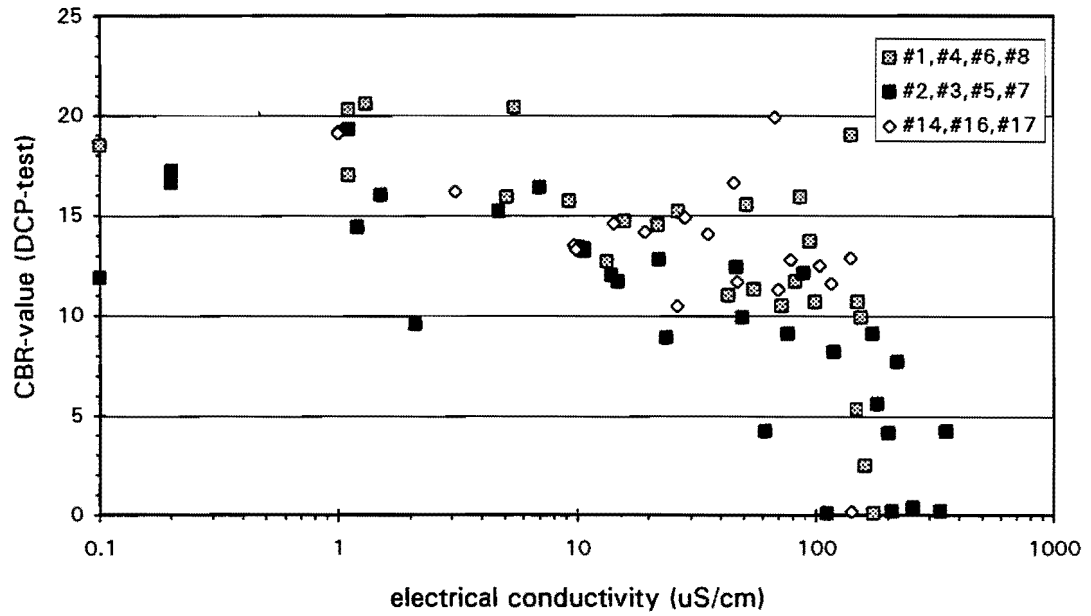


Figure 21. Correlation Between CBR-Value and Electrical Conductivity of Texas and Finnish Aggregates. Grey Squares Present Texas Carbonate Aggregates, Black Squares Other Texas Aggregates and Open Diamonds Finnish Aggregates.

- c. CBR-values are relatively high with low dielectric values, then stay at the same level. Changes in CBR-values are caused by the changes in the degree of compaction. These materials retain their strength properties even when the dielectric values are higher than 16, but in these cases, the material could not adsorb the added extra water and it was filtrating down to the bottom of the bucket. Thus these conditions do not represent realistic in situ conditions inside a highway base course. In these tests the only two non-plastic materials were samples #14 Tohmo granite and #17 Hietavaara gravel from Finland. Almost as good behavior was found with #8 Dolomite&Limestone gravel which had very high CBR-value at 10 % moisture content but then became slightly plastic at the moisture content of 12 %.

When looking at the CBR-value vs. electrical conductivity ratio (Figure 21) CBR-value stayed relatively stable until electrical conductivity values became greater than 100 $\mu\text{S}/\text{cm}$, and then the strength properties of aggregates dropped. The other results show that ion hydration might have a very important role in the strength properties of materials. The only material with linear negative correlation of conductivity and CBR-value was #5 Iron ore gravel, which had anomalous low conductivity values in all tests.

The hysteresis effect of wetting and drying to the strength and deformation properties of aggregates can be seen clearly in Figure 22, where the CBR-value vs. dielectric value of carbonate aggregates during wetting are plotted with the results measured during the drying cycle. The distributions of these results are the same as those published from the matric suction hysteresis (Fredlund and Rahardjo 1993, Lytton 1994) and explain how high resilient modulus values of the aggregates can be measured during the dry summer months.

Table 3 shows summary results from the resilient modulus tests. The influence of moisture content is clearly seen in both the measured surface dielectric and the K_1 term. The K_1 term is the dominant term in the universal equation presented in section 3.4 for computing the resilient modulus properties. Good quality bases are frequently measured to have K_1 values in excess of 800. In the wet state three of the bases tested had significantly low K_1 values, which results in a low moduli value. However, the results for aggregate #14 are different; even in the

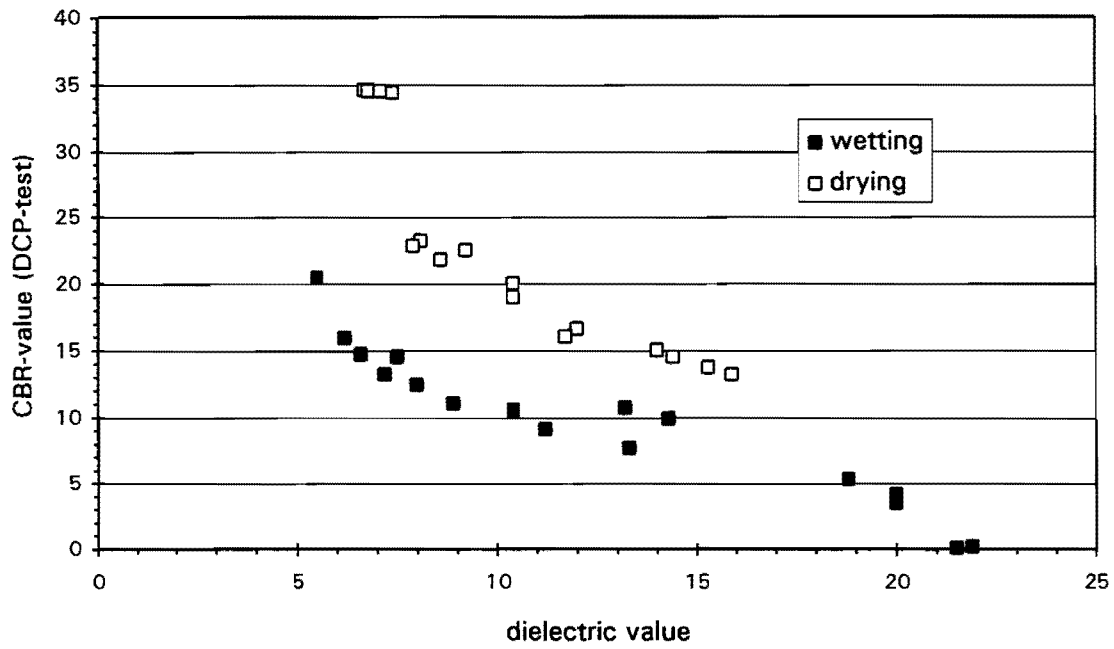


Figure 22. The Effect of Saturation and Drying in the Strength Properties and Dielectric Value of Texas Carbonate Aggregates.

Table 3. Resilient Modulus Test Results of the Test Aggregates.

| Material | Hyste- resis | moisture (%) by weight | dry dens. (g/cm ³) | dielectric value | electrical cond. (μ S/cm) | k1 | k2 | k3 |
|-------------|-----------------|------------------------------|--------------------------------------|---------------------|--------------------------------------|--------|----------|----------|
| #2 Gr./Bas. | wet | 7.0 | 2.28 | 17.9 | 50.4 | 456.3 | 0.00006 | -0.53665 |
| | dry | 4 | 2.18 | 8.5 | 224.0 | 1271.5 | 1.09624 | -0.70618 |
| #8 D/L Grav | wet | 8 | 2.2 | 12.3 | 75.1 | 469.9 | 2.4746 | -0.04541 |
| | dry | 3.6 | 2.2 | 8.6 | 59.7 | 3071.5 | 0.619774 | -0.26159 |
| #14 Granite | wet | 6 | 1.9 | 5.5 | 7.8 | 1167.5 | 0.472691 | -0.03412 |
| | dry | 0.9 | 1.9 | 3.1 | 0.9 | 2817.0 | 0.378879 | -0.10885 |
| #16 HW955 | wet | 7 | 2.3 | 14.3 | 129.3 | 201.4 | 0.815269 | -0.27329 |
| | dry | 2.3 | 2.3 | 6.3 | 8.3 | 8911.7 | 0.8237 | -0.26951 |

wet state the K_1 values were over 1000. It must be remembered that aggregate #14 was reported to be a very good performer in cold climates, whereas aggregate #16 was a poor performer reported to be moisture susceptible.

At any assumed stress condition within a typical pavement it is possible to use the Universal Equation to compute the resilient modulus of granular base materials. For all the aggregates tested, figures 23 shows the plot of resilient modulus against dielectric value. The only aggregate not to follow the trend was aggregate #14, which had very low water adsorption value and thus low suction properties. The trend is clear from this figure: dielectric values of 9 and below have high resilient moduli of over 50,000 psi. For dielectrics above 15, the moduli are very low, typically below 25,000 psi.

4.6. TUBE SUCTION TEST RESULTS

As a reference material, with a known low suction, a medium grained river sand was tested with the tube suction test (Figures 24 and 25). The results in the figures of dielectric value and electrical conductivity measurements show a distribution of values at different saturation levels. The river sand more than 200 mm above the water level remains dry indicating tightly bound adsorption water. Below the dry soil lies an interface zone, which could be called,

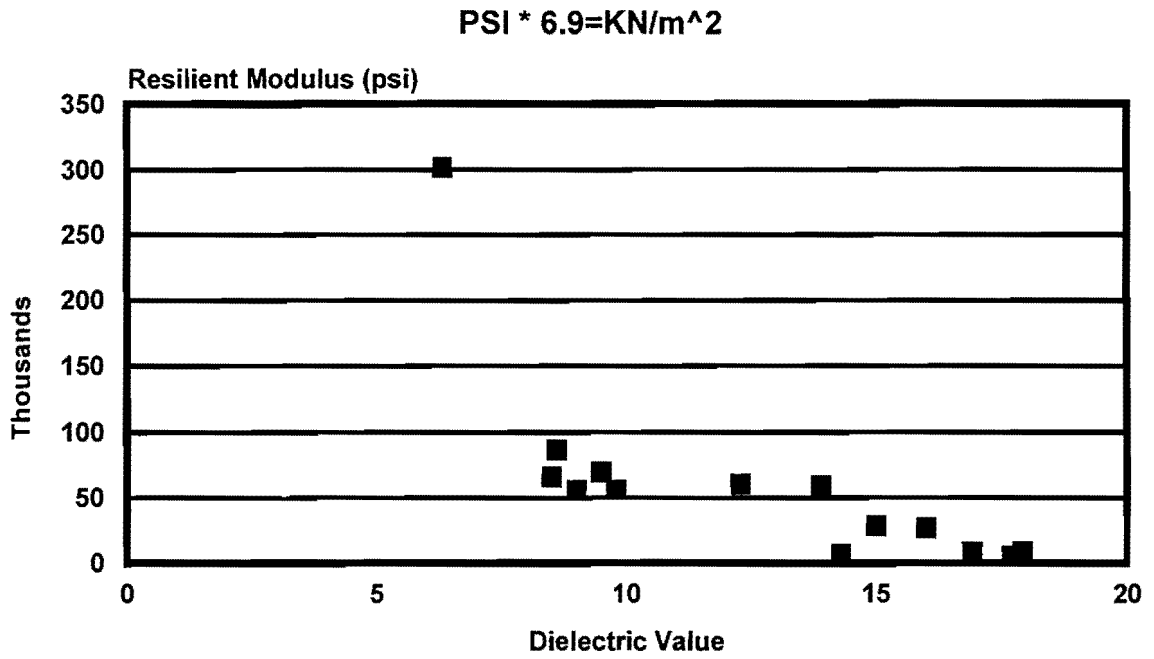


Figure 23. Correlation Between Dielectric Value and Resilient Modulus Calculated from Dynamic Triaxial Test of Test Aggregates.

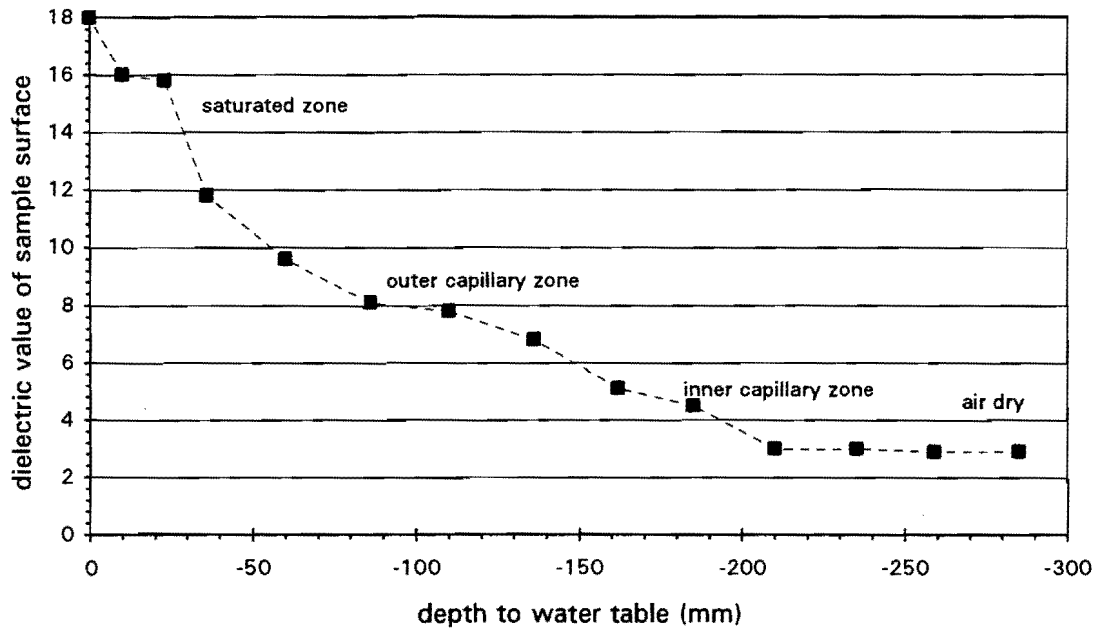


Figure 24. Dielectric Value Distribution Curve of Tube Suction Test of a Medium Grained Texas River Sand.

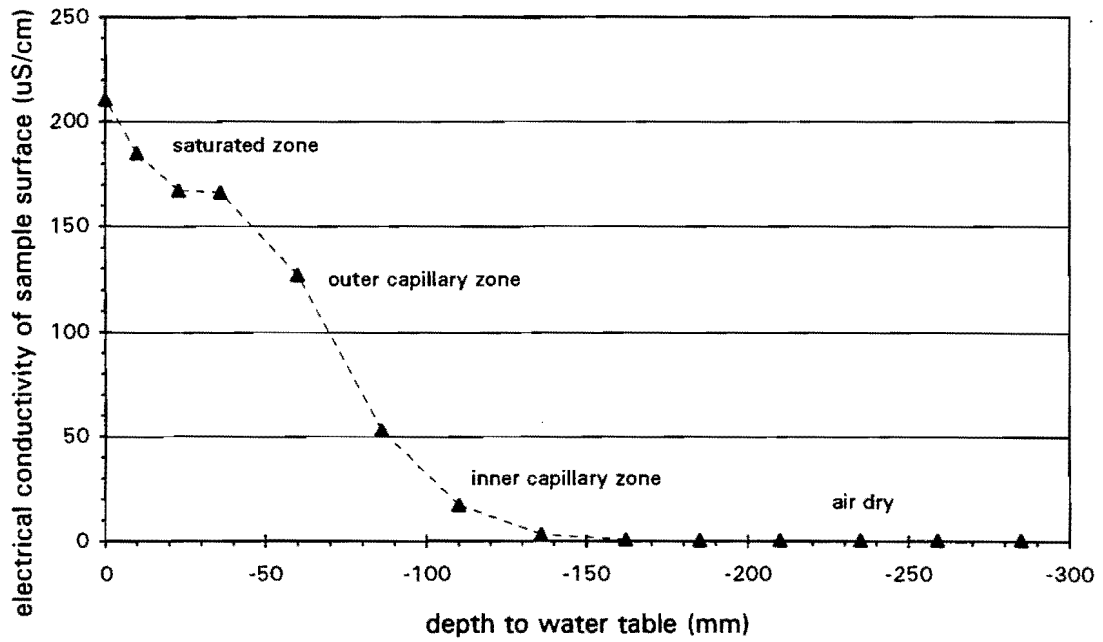


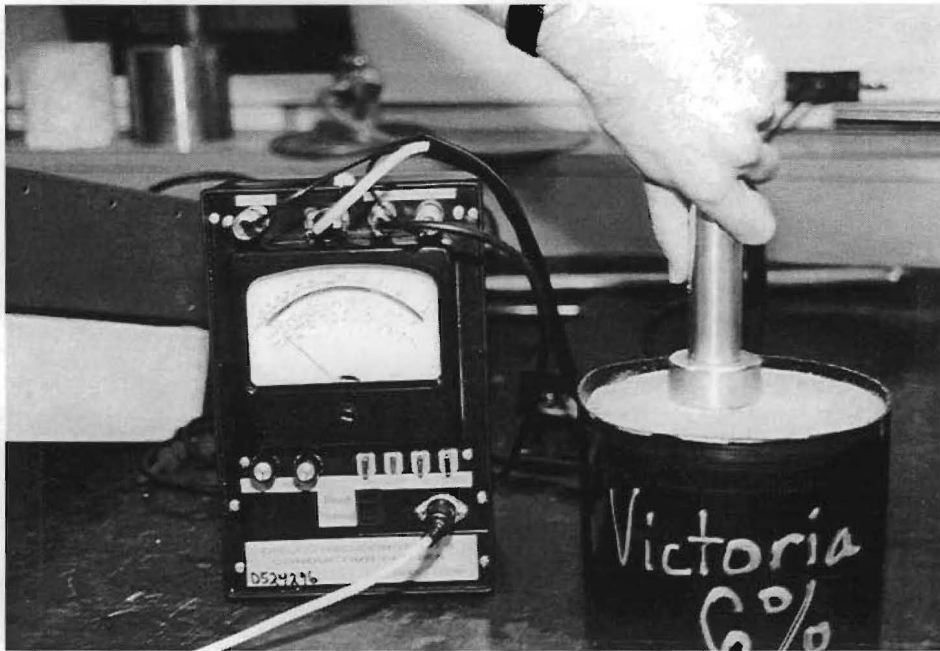
Figure 25. Electrical Conductivity Distribution Curve of Tube Suction Test of a Medium Grained Texas River Sand.

according to Lyon and Buckman (1937), inner capillary zone. In this zone the dielectric values start to rise, but electrical conductivities stay very low. The outer capillary zone, which corresponds to the actual capillary zone in soil mechanics, starts at the level of 120 mm above the water level, where the electrical conductivity starts to rise. From the level - 20 mm the dielectric and electrical conductivity values represent measurements on totally saturated material. The surface probe used to take these measurements measures to a depth of 20-25 mm; therefore, readings taken 20 mm above the saturated zone will be strongly influenced by that zone.

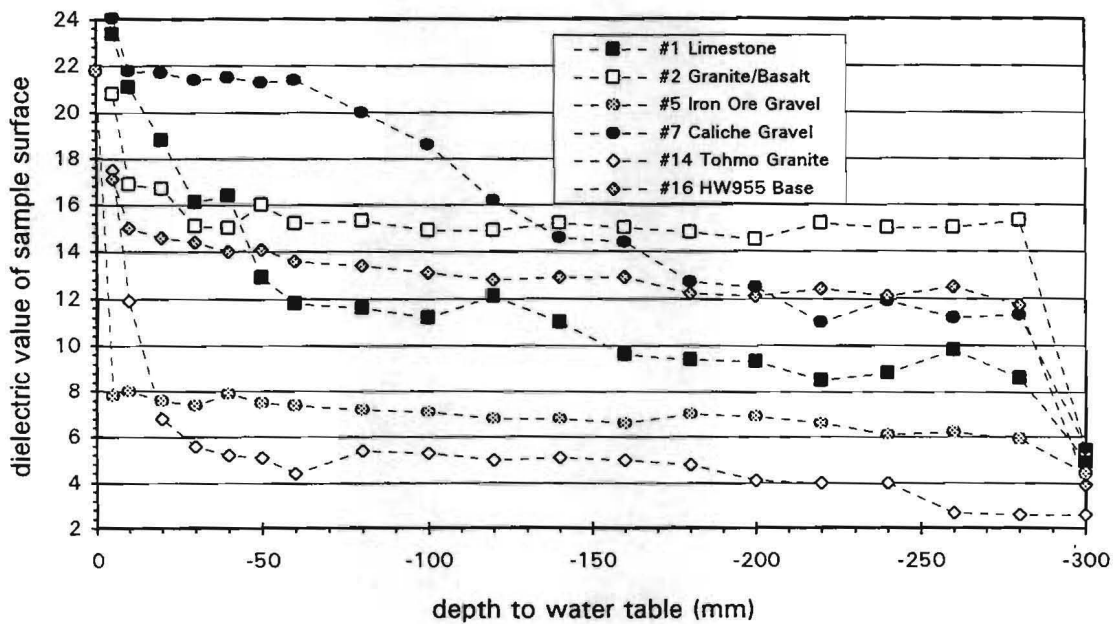
Figure 26 shows the surface dielectric probe and the results from the suction test on different aggregates. This test, as described earlier, involves standing the 300 mm high sample in 20 mm of water initially, and letting the sample come into equilibrium, then measuring the surface dielectric properties. The water level was then raised, and the test repeated. The lowest dielectric values were measured on samples #14 Tohmo granite and #5 Iron Ore Gravel which acted as an extremely hydrophobic materials. Texas carbonate aggregates were monitored to have high dielectric values at the level of -280 mm, but their dielectric values and water content increased markedly when the water level came near to the surface. Lowest dielectric values of the Texas carbonate aggregates were measured from sample #1 Limestone. The highest dielectric values at the water level of -280 mm were measured of sample #2 Granite/Basalt which was almost totally saturated at this level and dielectric values and water contents did not increase markedly after that. Similar behavior with slightly lower dielectric values was measured with the Finnish problem aggregate #16 HW955 base.

This test could potentially be an indicator test for aggregates that may perform poorly, particularly in cold climates. The hypothesis is that aggregate bases which strongly attract moisture will be susceptible to freeze/thaw and other damages. Poorly performing aggregates in this test are those that show rapid increase in surface dielectric between the -300 mm (dry state) and -280 mm depth (sample standing in 20 mm of water). These aggregate bases show marked increases in surface dielectric indicating high suction levels within the material. Samples #2, 16 and 7 were the worst performers in this test.

Researchers tested the effect of gradation on the suction properties with two aggregates #2 Granite/Basalt and #14 Tohmo granite, and Figure 27 presents the results. The grading of



a. Surface Probe



b. Surface Dielectrics Versus Depth to the Water Table.

Figure 26. Dielectric Surface Probe and the Results From the Suction Test.

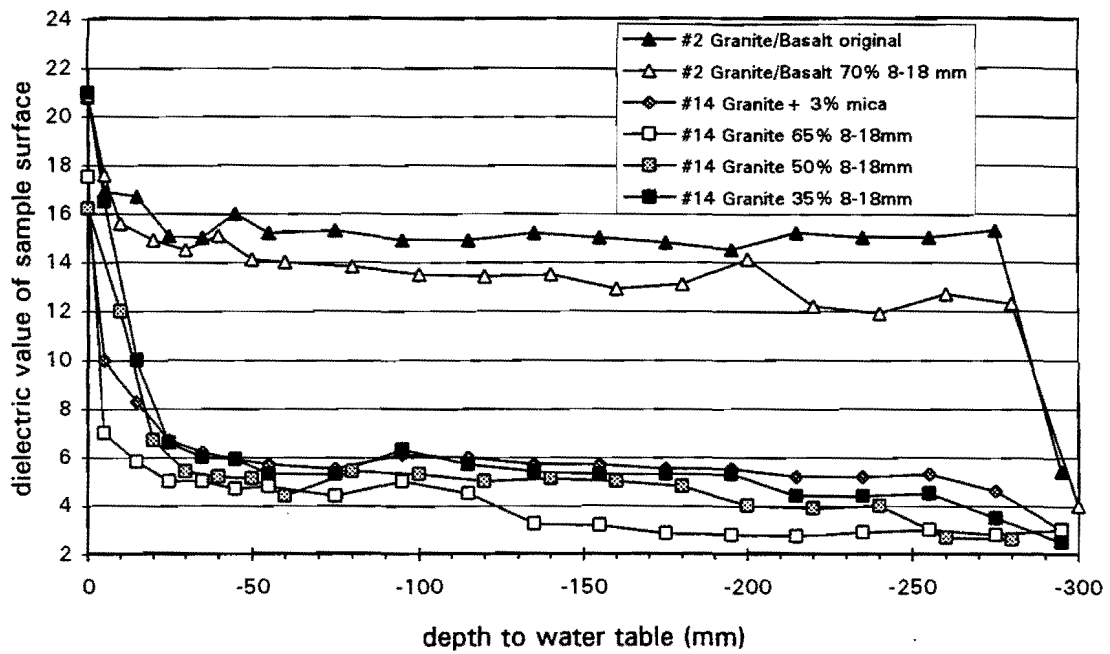


Figure 27. The Effect of Gradation to the Suction Properties of Samples #2 Granite/Basalt and #14 Tohmo Granite.

these aggregates has little effect on the suction, and materials with more fines have higher suction values. However, materials #2 and #14, with almost similar grading, have totally different suction level, and even the very coarse grained #2 Granite/Basalt has very high suction that it can totally saturate itself if water is available. This shows that electrochemical surface properties of the aggregate materials are the main factors influencing suction properties, and there is only limited possibility in reducing moisture sensitivity by changing grading of aggregate. The influence of chemical stabilization on suction properties should be the subject of future work in this area.

4.7. FREEZE/THAW EFFECT TO THE AGGREGATE PROPERTIES

The freeze/thaw test, even though the test set-up was not totally successful, gave very valuable information about the electrical properties of base aggregates during the freeze/thaw cycle. Figure 28 shows the relationship between dielectric properties of unfrozen and frozen aggregates before and after the freezing at the temperature of -5°C .

If the dielectric value of unfrozen base is higher than 9, it will cause the presence of unfrozen water in frozen aggregates, which causes suction and, according to Kujala (1991), is the greatest factor influencing the growth of ice lenses in materials. The dielectric limit value for the frost susceptible aggregates is, according to these results, about the same as for the frost susceptible soils (Saarenketo 1995b). When looking at electrical conductivity values in Figure 29, the electrical conductivities start to rise markedly if the corresponding values of unfrozen aggregates are higher than $150\ \mu\text{S}/\text{cm}$, which was also, according to the results presented in section 4.5, a limiting value for plastic behavior of aggregates. Sample #7 Caliche gravel presented anomalous behavior during the freezing test. Its dielectric value and electrical conductivity did not markedly change during the freezing test, which can be explained with extremely high electrical conductivity values. This reduces the freezing temperature and lowers the amount of free energy during the freezing process.

Figure 30 shows the dielectric values before and after the freeze/thaw cycle. The greatest increases of moisture were measured from the limestone aggregates #1 and #6 and the #16 HW955 base aggregate, which were all plastic 24 hours after the samples were taken out of the environmental room. The only sample with lower dielectric value after the freeze/thaw cycle was #5 Iron Ore Gravel.

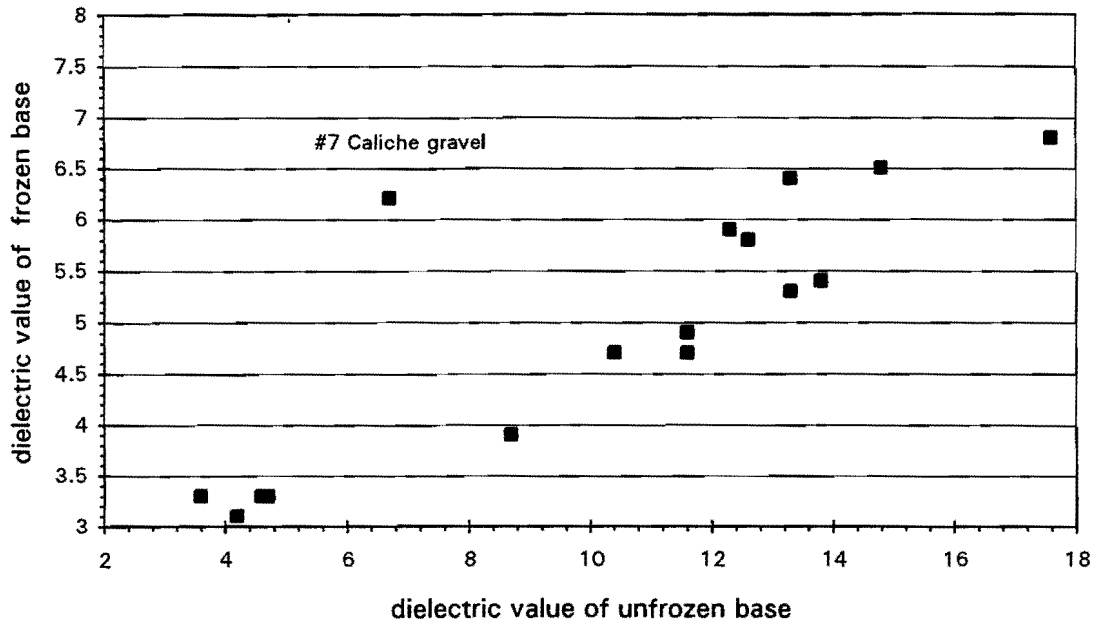


Figure 28. Correlation Between Dielectric Values of Unfrozen and Frozen Base Aggregates.

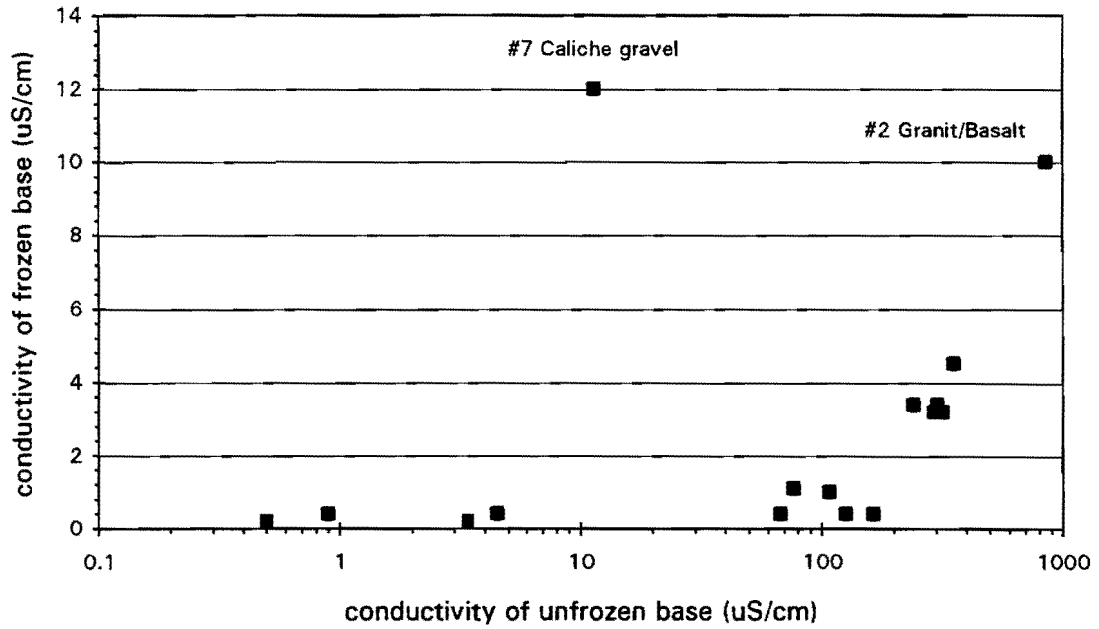


Figure 29. Correlation Between Electrical Conductivity Values of Unfrozen and Frozen Base Aggregates.

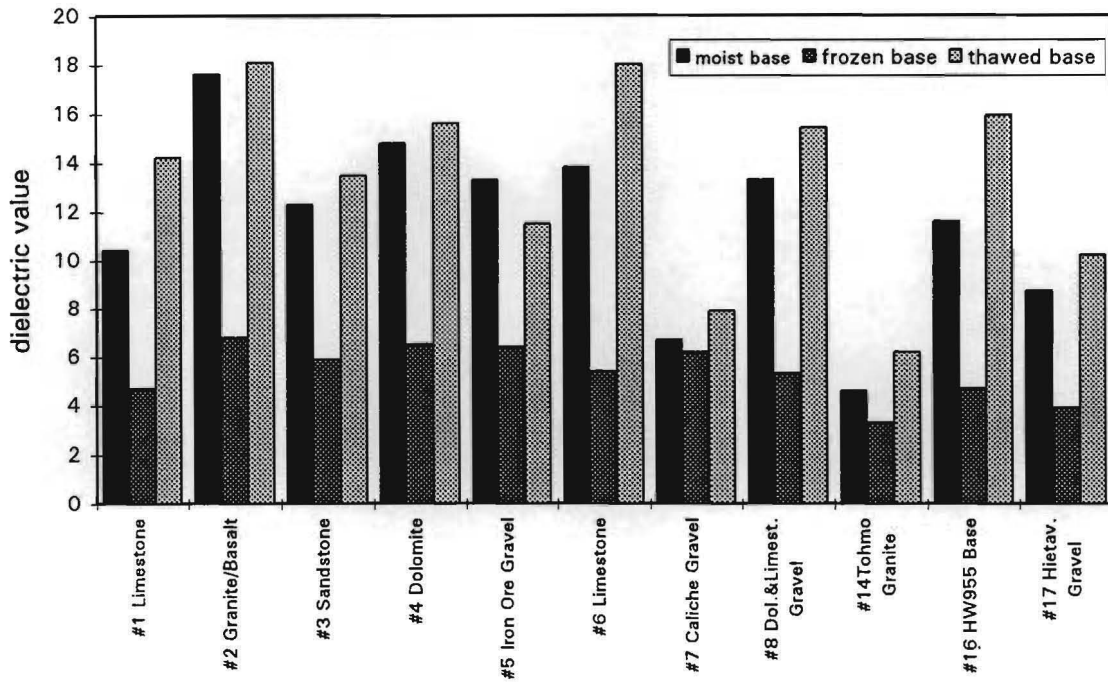


Figure 30. Dielectric Values of the Test Aggregates Before, During and After the Samples were Frozen at the Temperature of -5°C.

CHAPTER 5

CONCLUSIONS AND CLASSIFICATION OF BASE AGGREGATES ACCORDING TO THEIR ELECTRICAL PROPERTIES

Results of this survey show that dielectric value cannot be used directly to measure gravimetric water content or even the volumetric water content of the base course if the base material type is not known. However, according to the DCP and Resilient Modulus test results the dielectric value itself is a much better measure of the strength and deformation properties of road aggregates than the moisture content. High dielectric values, measured in the laboratory or field, are always good indicators of problems with that layer.

CBR-values calculated from DCP-test represent mainly the shear strength of the base course materials, while the dielectric values correlated with the tensile strength of the materials. The dielectric value itself is a measure of how well the water molecules are arranged around and between the aggregate mineral surfaces. High dielectric values indicate, in general, some kind of problem with the road materials or subgrade soils. DCP tests of the aggregates during the drying phase show that the role of grading on the strength properties has been surprisingly small and all the materials have followed almost identical curves, similar to the suction moisture curves, even though their grading differs markedly. The deviation of the CBR-values during the first bucket test when water was added can be partly explained by the changes in dry densities.

The effect of hysteresis and test results, especially of #5 Iron Ore Gravel and partly of #7 Caliche Gravel, show that the behavior of the material during the first compaction does not necessarily represent the final behavior of the material in highway base course. This is due to the many kinds of chemical reactions occurring when particle contacts form covalent and other types of bonds during the drying phase after the first compaction. In order to better simulate this self stabilization mechanism, the sample should be dried after compaction and then moisture should be introduced to the sample.

According to the test results, the strength and deformation behavior of aggregates can be simplified into three parts according to the moisture content:

1. At low moisture contents the large adsorption water content, with low dielectric values, causes tensile strength between particles, and thus, increases the strength of base layer under traffic loads. However "too low" dielectric values ($< 4.5 - 5$) indicate a lack of adsorption water, and the shear strength of the material is also lower. Rapid deformation can occur with open graded aggregates with no water adsorbing fines to improve the tensile strength of the material. Optimum dielectric value range for base materials is about 5 - 6.5.
2. When adsorption water layers are filled at higher moisture contents the strength of the base is mainly based on the friction properties of the material, but also suction and hysteresis have a great effect in this moisture range.
3. At high volumetric water contents, ions are dissociated in free water and at the same time forming an immobilized zone of water, which acts as a bound adsorption layer. The hydrated radius is especially large in alkaline earths (Ca^{2+} : 9.6 Å and Mg^{2+} : 10.8 Å). If the base material has too many ions available to dissociate to water, under a dynamic load these "water adsorbing" ions can cause interparticle repulsion or they can block the interparticle pores so that free polar water cannot penetrate them. This causes positive pore pressure, and the strength of the structure will collapse. However, all of the factors in this process are not yet totally clear to the authors, and this needs still more research work.

In general, dielectric values provide information about the position of the material in the aggregate moisture range, and electrical conductivity gives information about whether the material is on drying or wetting cycle. High electrical conductivity values indicate loss of strength of base course. Tentative guidelines for interpreting these electrical properties in terms of their anticipated strength and performance are given in Table 4. It is important to remember that GPR can measure both of these values non-destructively and continuously. Water sensitive base aggregates can be identified even when they are dry from their dielectric dispersion properties. This can be done by using at least two GPR frequencies when measuring base course thickness and quality and/or comparing dielectric values or by studying changes in the reflected signal frequency response. The results of these surveys can direct the strength testing

Table 4. Classification of Base Aggregates According to Their Electrical Properties.

| Dielectric value | Electrical conductivity ($\mu\text{S/cm}$) | Material | Strength and deformation properties | Frost susceptibility and water sensitivity |
|------------------|--|---|--|---|
| <5 | < 10 | -dry and open graded base with low water adsorption and large air - solid ratio | -low tensile strength, might be sensitive to permanent deformation by compaction | -non frost susceptible, non water sensitive |
| 5 - 6.5 | < 50 | -dry base with low water adsorption value and optimum dry density | -optimum strength properties | -non frost susceptible, non water sensitive |
| 6.5 - 9 | < 100 | -slightly moist base with high suction value | -high shear strength because of suction, hysteresis has great effect on strength value | -might become water sensitive and frost susceptible if drainage stops working |
| 9 - 16 | < 150 | -moist base | -reduced shear strength because of reduced suction | -frost susceptible and water sensitive |
| > 16 | < 150 | -wet or water saturated base | -adequate shear strength , no positive pore water pressure under dynamic load | -may form ice lenses |
| > 16 | > 150 | -wet or water saturated base | -under a dynamic load plastic deformation may occur because of high pore water pressure and low shear strength | -extremely frost susceptible |

equipment, such as the Falling Weight Deflectometer, to the most critical parts of the road and reduce the error when back calculating the layer modulus values.

These test results show that all of the eight Texas aggregates and one of three Finnish studied aggregates are sensitive to moisture. Positive pore water pressure formed in all tests causing plastic deformation at high moisture contents. All the Texas aggregates had high specific surface area and water adsorption values, and they produced even more of these water adsorbing fines during the compaction. These types of material behave well - and may even appear structurally superior to aggregates with lower water adsorption values - when the road drainage works well and base course is dry. In hot and dry summer months, extremely high bearing capacity values can be expected from these aggregates. However, if the structure gets

moisture through pavement cracks, or by suction from road shoulders or from the subgrade, the road can deteriorate very rapidly under traffic load. Furthermore the freeze/thaw phenomenon may cause performance problems with these aggregates. Freeze/thaw causes moisture flow to the top of the base course, and this can cause thermal cracking and/or weakening of the upper part of the base layer.

REFERENCES

AASHTO Guide for Design of Pavement Structures, American Association of State Highway and Transportation Officials, Washington, 1986.

Anderson, T.M. 1989. Frost heave properties of soils. In Frost in geotechnical engineering. Volume 1. International Symposium, Saariselkä, Finland, Ed. by Hans Rathmayer. Espoo 1989. pp. 105-125

Annan, A.P., Davis, J.L. and Scott, W.J. 1975. Impulse Radar Wide Angle Reflection and Refraction Sounding in Permafrost. Geological Survey of Canada, Paper 75-1C. pp. 335-341.

Arulanandan, K., Smith, S.S. and Spiegler, K.S. 1973. Soil structure evaluation by the use of radio frequency Electrical dispersion. Proceedings of the International Symposium on Soil Structure, Gothenburg, Sweden. pp. 29-49.

Campbell, J.E. 1990. Dielectric properties and influence of conductivity in soils at one to fifty Megahertz. Soil. Sci. Soc. Am. J. 54. pp. 332-341.

Carpenter, S.H. and Lytton, R.L. 1977. Thermal Pavement Cracking in West Texas. Texas Transportation Institute Research Report 18-4F, Study 2-8-73-18. Texas A&M University, College Station, Texas. p. 232.

Daniels, D.J., Gunton, D.J. and Scott, H.F. 1988. Introduction to subsurface radar. IEE Proceedings Vol. 135, PtF, No. 4, Communication, Radar and Signal Processing 135 F. pp. 278-320.

Davis, J.L. and Annan, A.P. 1989. Ground-Penetrating Radar for High Resolution Mapping of Soil and Rock Stratigraphy. Geophysical Prospecting 37, pp. 531-551.

Dobson, M.C., Ulaby, F.T., Hallikainen, M.T. and El-Rayes, M.A. 1985. Microwave dielectric behaviour of wet Soil - Part II: Dielectric Mixing Models. IEE Transaction on Geoscience and Remote Sensing GE-s3 (1). pp. 35-46.

Fredlund, D.G. and Rahardjo, H. 1993. Soil Mechanics for Unsaturated Soils, John Wiley & Sons, New York. p.517.

Fredlund, D.G., Gan, J.K-M. and Gallen, P. 1995. Suction Measurements on Compacted Till Specimens and Indirect Filter Paper Calibration Technique. Transportation Research Board Paper 950891.

Ground Penetrating Radar (1992). Geophysical Research Methods. The Finnish Geotechnical Society and The Finnish Building Centre Ltd.

Hudec, P.P. and Achampong, F. 1994. Improving Aggregate Quality by Chemical Treatment. Report on the 2nd International Aggregates Symposium, Erlangen, Germany, Ed. by G.W. Luttig. pp. 135-146.

Knight, R. and Knoll, M. 1990. The effect of saturation history on electrical properties of the unsaturated zone. Third International Conference on Ground Penetrating Radar. Abstracts of the technical meeting. US Geological Survey, Lakewood, Colorado, USA. p. 42.

Knoll, M.D. and Knight, R. 1994. Relationship Between Dielectric and Hydrogeologic Properties of Sand-Clay Mixtures. In Proceedings of The Fifth International Conference on Ground Penetrating Radar, June 12-16, Kitchener, Ontario, Canada, Vol 1 of 3. pp. 45-61.

Kolisoja, P. 1993. Deformation properties of aggregates of unbound layers. Literature research. Finnish National Road Administration. FinnRA Reports b38/1993, TIEL 3200163. English abstract. p. 147.

Konrad, J.M. and Morgenstern, N.R. 1980. A mechanistic theory of ice formation in fine grained soils. *Can. Geotech. J.* 17. pp. 473-486.

Kujala, K. 1991. Factors affecting frost susceptibility and heaving pressure in soils. *Acta Univ. Oul. Series C. Technica* 58. p. 99.

Ladanyi, B. and Shen, M. 1989. Mechanics of Freezing and Thawing in Soils. In *Frost in Geotechnical Engineering. Volume 1. International Symposium, Saariselkä, Finland, 13-15.* Ed. by Hans Rathmayer. Espoo. pp.73-103.

Lau, C.L. 1991. Thickness Assessment Using GPR, Thesis for Master's Degree in Electrical Engineering, Texas A&M University, College Station, Texas.

Lau, C.L, Scullion, T. and Chan, P. 1992. Using Ground Penetrating Radar technology for pavement evaluations in Texas, USA. *Geological Survey of Finland, Special Paper* pp. 16, 277-283.

Lyon, T.L. and Buckman, H.O. 1937. *The Nature and Properties of Soils.* The Macmillan Company, New York. p. 391.

Lytton, R.L. 1994. Prediction of Movement in Expansive Clays. *Geotechnical Special Publications No. 40. "Vertical and Horizontal Deformations of Foundations and Embankments."* Ed. A. Young, American Society of Civil Engineers.

Marjeta, J. 1993. Dielektrisyysmittarin käyttö murskeiden kosteuksen mittaukseen ja murskeiden laadun arviointiin. *Insinööriyö, Rovaniemi Institute of Technology, Department of Construction technology.* English Abstract: The Use of dielectric permittivity meter in moisture and qualitative determination of crushed gravel. p. 55.

Maijala, P., Saarenketo, T. and Valtanen, P. 1994. Correlation of Some Parameters in GPR Measurement data with Quality Properties of Pavements and Bridge Decks. Proceedings of Fifth International Conference on Ground Penetrating Radar, Kitchener, Ontario, Canada. Waterloo Centre for Ground water Research. pp. 393-406.

Maser, K.R. and Scullion, T. 1991. Automated Detection of Pavement Layer Thicknesses and Subsurface Moisture Using Ground Penetrating Radar. Transportation Research Board Paper, Washington, D.C.

Maser, K.R., Scullion, T. and Briggs, R.C. 1991. Use of Radar Technology for Pavement Layer Evaluation. Research Report 930-5F. Texas Transportation Institute, College Station, Texas. p.19.

Mitchell, J.K. 1992. Fundamentals of Soil Behaviour. Second Edition. John Wiley & Sons, New York. p. 437.

Plakk, T. 1994. HF Permittivity measurements by capacitive probe. Unpublished article. Adek Ltd, Uus-Saku, Estonia.

Ravaska, O. and Saarenketo, T. 1993 Dielectric properties of road aggregates and their effect on GPR surveys. Proc. 2nd Int. Symp. on Frost in Geotechn. Eng., Anchorage, USA. Balkema. pp. 17-22.

Saarenketo, T. 1992. Ground Penetrating Radar Applications in Road Design and Construction in Finnish Lapland. Geological Survey of Finland, Special paper 15, pp. 161-167.

Saarenketo, T. 1994. Dielektrisyys- ja sähköjohtokykykymittausten käyttö pohjamaan routivuuden luokitteluun. Aloite 12.4. FinnRA, Road District of Lapland, p.26 (In Finnish).

Saarenketo, T. 1995a. Using Electrical Methods to Classify the Strength Properties of Texas and Finnish Base Course Aggregates. Center for Aggregates Research, 3rd Annual Symposium Proceedings, Austin, Texas. p.19.

Saarenketo, T. 1995b. The Use of Electric and Electrical Conductivity Measurements and Ground Penetrating Radar for Frost Susceptibility Evaluations of Subgrade Soils. Proceedings of the Symposium on the Application of Geophysics to Engineering and Environmental problems. Compiled by Ronald S. Bell. Orlando, Florida. pp.73-85.

Saarenketo, T. and Nieminen, P. 1989. Frost damage in road materials in Kittilä, Northern Finland. Proceedings of Frost in Geotechnical Engineering. Vol 2. International Symposium, Saariselkä, Finland, Espoo. Ed. by H. Rathmayer. pp. 709-720.

Saarenketo, T. and Söderqvist, M-K. 1993. GPR Applications in Bridge Deck Evaluations in Finland. Proceedings of The Non-Destructive Testing in Civil Engineering. Ed. by J. Bungey. The University of Liverpool. pp. 211-226.

Saarenketo, T. and Scullion, T. 1994. Ground Penetrating Radar Applications on Roads and Highways. Research Report 1923-2F. Texas Transportation Institute, College Station, Texas. p. 36.

Scullion, T., Lau, C.L. and Chen, Y. 1992 Implementation of the Texas Ground Penetrating Radar System. Research Report 1233-1. Texas Transportation Institute, College Station, Texas. p. 80.

Sutinen, R. 1992. Glacial deposits, their electrical properties and surveying by image interpretation and ground penetrating radar. Geological Survey of Finland, Bulletin 359. p. 123.

Sutinen, R. and Hänninen, P. 1990. Radar profiling and dielectrical properties of glacial deposits in North Finland. Proc. 6th International IAEG Congress, Amsterdam, 2, pp. 1045 - 1051.

Sweere, G.T.H. 1990. Unbound granular bases for roads. Ph.D. thesis, Delft University of Technology, Delft, Netherlands. p. 384.

Thom, N.H. 1988. Design of Road Foundations. Ph.D Thesis, Department of Civil Engineering, University of Nottingham, England.

Titus-Glover, L., and Fernando, E.G. 1995. "Evaluation of Pavement Base and Subgrade Material Properties and Test Procedures," Report 1335-2, Texas Transportation Institute, College Station, Texas.

Tsytovic, N.A. 1986. The mechanics of frozen ground. Ed. by Swinzow. Scripta Book Company and McGraw-Hill Book Company, Washington D.C. p. 426.

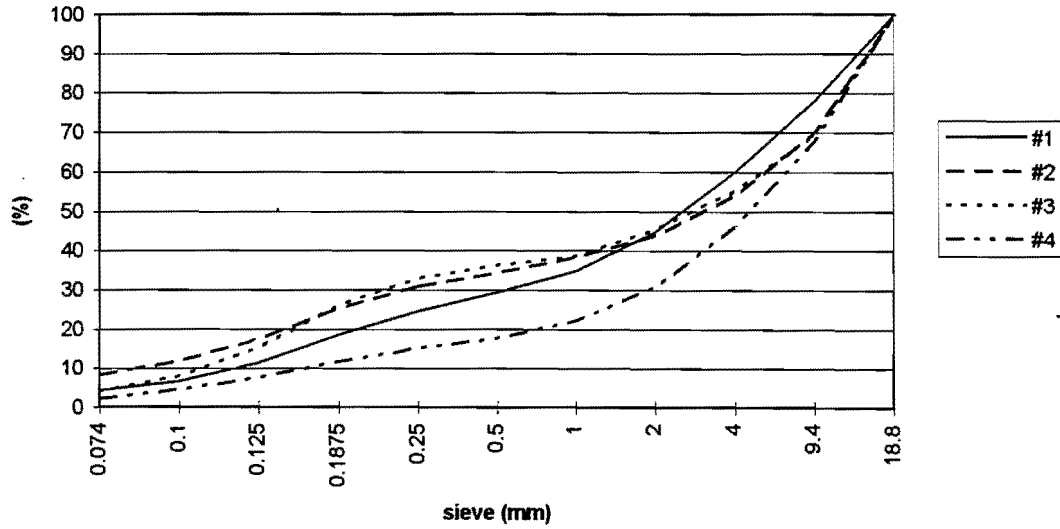
Ulriksen, C.P.F. 1992. Application of Impulse Radar to Civil Engineering. Doctoral Thesis. Lund University of Technology. Department of Engineering Geology, Sweden. p. 179.

Uzan, J. 1985. Characterization of Granular Materials, Analysis and Testing of Granular Bases and Subbases. In *Transportation Research Record* 1022, Transportation Research Board, National Research Council, Washington, D.C. pp. 52-59.

Webster, S.L., Graw, R.H. and Williams, T.R. 1992. Description and Application of Dual Mass Dynamic Cone Penetrometer" Report GL-92-3. USAE Waterways Expt Station, Vicksburg, MS 39180-6199.

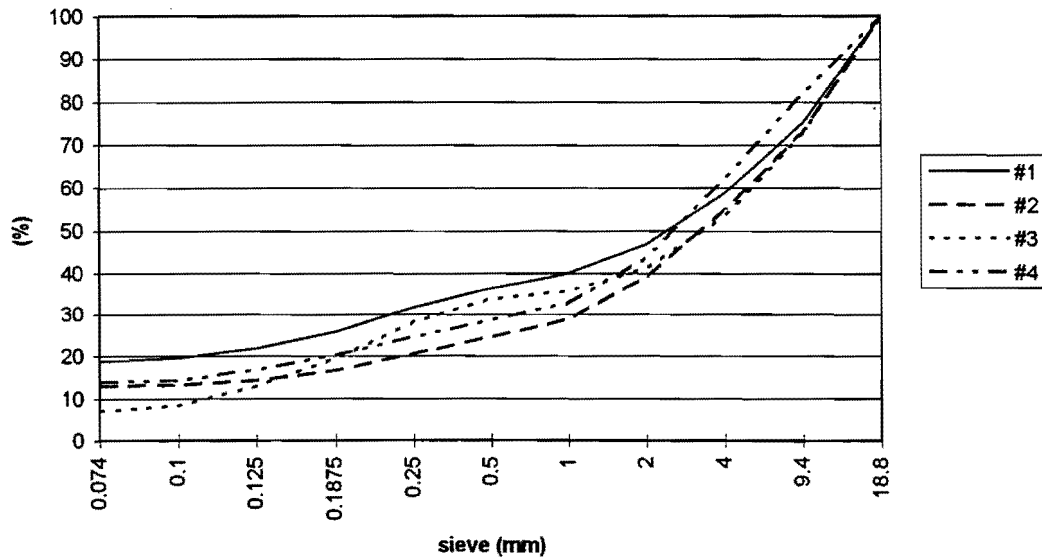
APPENDIX
GRAIN SIZE DISTRIBUTION CURVES
OF TESTED TEXAS AGGREGATES

Grain Size Distribution of Texas Aggregates #1-4 (<18.8 mm)



a) Before Bucket Test

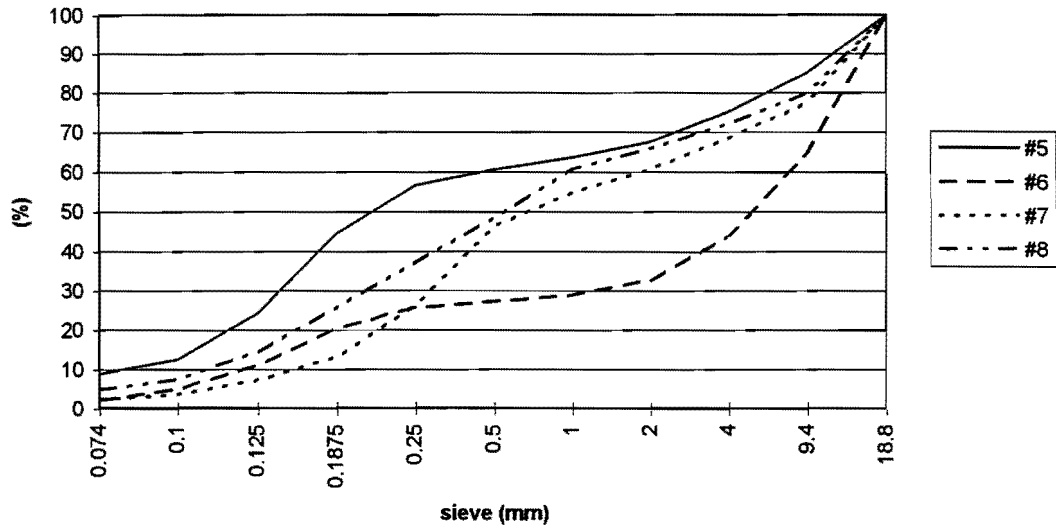
Grain Size Distribution of Texas Aggregates #1-4 After Bucket Test



b) After Bucket Test

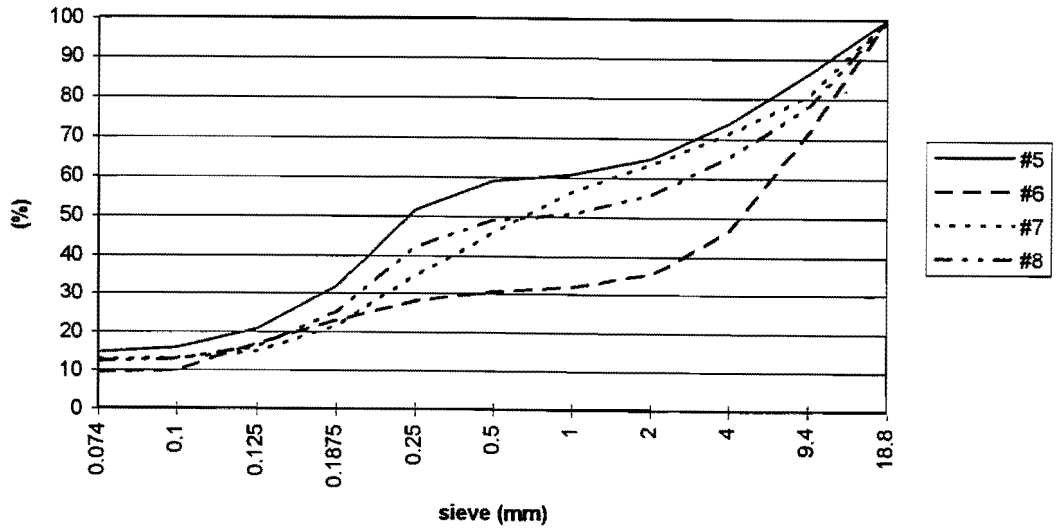
Figure A1. Grain Size Distribution of Texas Aggregates #1-4.

Grain Size Distribution of Texas Aggregates #5-8 (<18.8 mm)



a) Before Bucket Test

Grain Size Distribution of Texas Aggregates #5-8 After Bucket Test



b) After Bucket Test

Figure A2. Grain Size Distribution of Texas Aggregates #5-8.

